


ORIGINAL ARTICLE

Dopamine D₂R is Required for Hippocampal-dependent Memory and Plasticity at the CA3-CA1 Synapse

Isabel Espadas^{1,2}, Oscar Ortiz^{1,2}, Patricia García-Sanz^{1,2}, Adrián Sanz-Magro^{1,2}, Samuel Alberquilla^{1,2}, Oscar Solis^{1,2}, José María Delgado-García³, Agnès Gruart³ and Rosario Moratalla^{1,2} 

¹Neurobiología Funcional y de Sistemas, Instituto Cajal, CSIC, Madrid 28002, Spain, ²CIBERNED, ISCIII, Madrid 28002, Spain and ³División de Neurociencias, Univ. Pablo de Olavide, Sevilla 41013, Spain

Address correspondence to Dr. Rosario Moratalla, Instituto Cajal, CSIC, Avda Dr Arce, 37, Madrid 28002, Spain. Email: moratalla@cajal.csic.es.

Abstract

Dopamine receptors play an important role in motivational, emotional, and motor responses. In addition, growing evidence suggests a key role of hippocampal dopamine receptors in learning and memory. It is well known that associative learning and synaptic plasticity of CA3-CA1 requires the dopamine D₁ receptor (D₁R). However, the specific role of the dopamine D₂ receptor (D₂R) on memory-related neuroplasticity processes is still undefined. Here, by using two models of D₂R loss, D₂R knockout mice (*Drd2*^{-/-}) and mice with intrahippocampal injections of *Drd2*-small interfering RNA (*Drd2*-siRNA), we aimed to investigate how D₂R is involved in learning and memory as well as in long-term potentiation of the hippocampus. Our studies revealed that the genetic inactivation of D₂R impaired the spatial memory, associative learning, and the classical conditioning of eyelid responses. Similarly, deletion of D₂R reduced the activity-dependent synaptic plasticity in the hippocampal CA1-CA3 synapse. Our results demonstrate the first direct evidence that D₂R is essential in behaving mice for trace eye blink conditioning and associated changes in hippocampal synaptic strength. Taken together, these results indicate a key role of D₂R in regulating hippocampal plasticity changes and, in consequence, acquisition and consolidation of spatial and associative forms of memory.

Key words: *Drd2*^{-/-}, hippocampal, learning, long-term potentiation, memory

Introduction

Dopamine is one of the main neurotransmitters in the brain, involved in neuroendocrine, motivational/emotional, motor, and cognitive functions. Dopaminergic fibers innervate structures such as hippocampus, prefrontal cortex, striatum, and amygdala. The hippocampal region receives dopaminergic fibers originated from the ventral tegmental area, substantia nigra, and locus coeruleus (Bethus et al. 2010; Smith and Greene 2012; Nguyen et al. 2014; Takeuchi et al. 2016; Edelmann and Lessmann 2018). Early evidence demonstrates that dopamine

release in the hippocampus is required for learning and memory (McNamara et al. 2014; Rosen et al. 2015; Broussard et al. 2016). In support of this, several studies on Parkinson's disease (PD) patients recognized a prodromal phase with critically impaired cognition before the development of motor symptoms, particularly executive functions, spatial, and complex associative learnings (Weintraub et al. 2015; Aarsland et al. 2017; Grogan et al. 2018).

Similar cognitive deficits have been found in animal models of PD. MPTP-treated monkeys fail in operant task performances

of visual discrimination (Schneider and Roeltgen 1993) and 6-OHDA-lesioned rats are impaired in the Morris water maze (MWM), two-way active avoidance and spatial discrimination (Da Cunha et al. 2002; Mura and Feldon 2003; De Leonibus et al. 2007). Likewise, dopamine-deficient mutant mice (DD-mice) have impaired spatial, procedural, and associative learning (Darvas and Palmiter 2009, 2010; Fadok et al. 2009; Darvas et al. 2011).

Dopamine receptors are critical in these processes. Previous works from our laboratory using dopamine D₁R knockout mice (*Drd1a*^{-/-}) and others using D₁R antagonists evidenced similarities with DD-mice. D₁R inactivation with constitutive knock-out mice or pharmacological blockade in the hippocampus impaired spatial, associative and episodic-like memory, altered early long-term potentiation (E-LTP) and late LTP (L-LTP), and decrease their maintenance by disturbing the transition from one to the other (O'Carroll et al. 2006; Granado et al. 2008; Bethus et al. 2010; Ortiz et al. 2010; Wang et al. 2010; Takeuchi et al. 2016). In addition, these alterations correlate with a severe decrease in the expression of hippocampal CA1 ARC and Zif268 genes (El-Ghundi et al. 1999; Granado et al. 2008; Ortiz et al. 2010) suggesting a critical role in the regulation of transcriptional processes that are essential for memory consolidation.

Because the affinity of D₁R for dopamine is lower than that of D₂R (Wall et al. 2011), it was suggested that D₁R would only be activated with temporary increases in dopamine (Goto and Grace 2005; Grace et al. 2007; Wall et al. 2011), while D₂R would be involved in mediating the tonic effects of dopamine (Goto et al. 2007; Wall et al. 2011). The activation of D₂R would act as a gating signal indicating when new information should be encoded and maintained, or when an update of current representations is needed (Glickstein et al. 2002).

Previous studies have shown D₂R expression in dentate gyrus and CA1-stratum radiatum and stratum lacunosum moleculare of mice (Higuera-Matas et al. 2010; Gangarossa et al. 2012; Rocchetti et al. 2015; Wei et al. 2018) and humans (Nyberg et al. 2016). Furthermore, D₂R density decrease in different brain regions, including the hippocampus, correlated with cognitive dysfunctions in PD, Alzheimer's disease, and dementia with Lewy bodies (Kempainen et al. 2003; Tanaka et al. 2003; Piggott et al. 2007; Christopher et al. 2014, 2015). However, little is known about the specific role of D₂R for hippocampal-dependent memory processes.

The aim of this study is to unravel the role of D₂R in associative and spatial learning and memory processes. To address this, we used genetically modified mice with the inactivation of D₂R (*Drd2*^{-/-}) and the specific silencing of this receptor in the hippocampus by *Drd2*-small interfering RNA (*Drd2*-siRNA). Our results show that the absence of D₂R impairs acquisition and consolidation of hippocampal-dependent processes in associative and spatial learning. In addition, the complete loss of D₂R, as well as its specific silencing in CA1 by siRNAs, significantly reduces the acquisition of trace eyeblink conditioned responses. These results are also supported by a significant reduction of the synaptic strength at the CA3-CA1 synapses in the hippocampus.

Material and Methods

Animals

C57BL/6 and *Drd2*^{-/-} mice were used for this study. The mating of heterozygous mice resulted in offspring including male and female wild-type (WT) and homozygote *Drd2*^{-/-} mice. For all of

our studies, we used mice between 3- and 6-month-old (25–30 g). Genotype was determined by PCR analysis (Solis et al. 2019).

Groups of 6 mice per cage were kept in at 22 °C on a 12 h dark–light cycle, and were given free access to food and water. All animal experiments were conducted as per European Community guidelines (2010/63/EU), and the Bioethical Committee at the Cajal Institute approved all procedures.

Spatial Learning

Morris Water Maze

Spatial learning and memory were assessed in *Drd2*^{-/-} mice (*n* = 24) and WT (*n* = 24) littermates using the MWM as described previously (Granado et al. 2008). The maze consisted of a circular tank (100 cm diameter) filled with 21 °C water located in a room with visible external cues. During the acquisition trials (days 1 to 14), mice were trained to escape from the water by swimming from variable starting points around the tank to a hidden platform, and allowed to remain there for 15 s. Mice that failed to find the platform within 60 s were guided to the platform and placed on it for 15 s. After each trial, mice were dried and returned to their home cages. All sessions were recorded by a video camera located above the tank. Mice received four trials per day, for 14 consecutive days, with an inter-trial interval of 5–7 min, and their escape latency was recorded for each trial. Probe trials (no platform) were performed on the first day (day 1, short-term retention) and 72 h after the last acquisition trial (day 17, long-term retention memory), where mice were allowed to swim for 60 s. The swimming speed and the amount of time each mouse spent in the target quadrant were recorded. Reversal trials were conducted with all mice after the second probe trial on day 17; these trials had the hidden platform located diagonally to the previous position. Four trials were conducted per day, over three consecutive days (days 17–19), for a total of 12 trials, and escape latencies were recorded.

In an additional experiment, cued training trials were performed. Mice were trained to locate a submerged platform marked with a local visible cue. These training trials tested their non-spatial learning ability, motivation, and sensorimotor coordination. All mice were subjected to 8 trials over 2 consecutive days.

Associative Learning

Active Avoidance

For this test, we used a 2-way shuttle-box (AccuScan Instruments, Inc. Columbus, Ohio) with acrylic walls and stainless-steel bars in the floor controlled by a programming/recording unit with a shock generator (AccuScan Instruments, Inc.) as described previously (Ortiz et al. 2010). Mice (*n* = 10 per group) received a single training session once a day for 8 days consecutively. Each session comprised a 3-min adaptation period where the mice were allowed to move freely between the compartments, followed by 20 trials separated by a 20-s intertrial interval (±5 s to avoid any time associations). During each trial, a red light and a tone (100 GHz, 100 dB) were simultaneously presented for 10 s (the conditioned stimulus; CS) in the compartment where the animal was located. After 5 s of the CS, a 0.2-mA electric foot-shock was applied (unconditioned stimulus; US) for up to 10 s. If the mouse moved to the other compartment after the CS but before the US, this was recorded as an “avoidance” response. If the mouse moved to the other compartment during the delivery of the shock, this was recorded as an “escape” response. The time (in seconds) from the start of

the CS to when the mouse moved to the opposite compartment was recorded as the response latency. The number of times the mouse crossed between the compartments during the intertrial interval was used to measure the general activity. Three days after the training phase was completed (day 11), the test session was performed. Before and after each mouse was tested, the apparatus was cleaned with 70% ethanol to remove any residual odors.

Passive Avoidance

This test was conducted as previously described (Pittenger et al. 2006; Ortiz et al. 2010). Mice ($n=10$ per group) were placed into the passive avoidance box (Ugo Basile, Rome, Italy) with two different compartments, one dark and the other illuminated and white. On the first test day, we measured the time that the mice spent in the white compartment. As soon as the animal crossed into the black compartment, the automatic door was closed and mice received an electrical foot-shock (0.4 mA, 1 s). The test was repeated 1 and 24 h after the foot-shock, in the same conditions but without the foot-shock to measure short-term and long-term memory retention.

Contextual Fear Conditioning and Extinction

To assess contextual fear conditioning (CFC), we used a fear conditioning task as previously described (Alarcón et al. 2004; Ortiz et al. 2010). On the training day, mice were placed in the conditioning chamber for 2 min before onset of the CS (a 30-s tone). During the last 2 s, the US (an electrical shock) was paired with the CS. Mice were kept in the chamber for an additional 30 s before being returned to the home cage. Conditioning was evaluated 24 h later by measuring the freezing behavior with a tracking video system (Panlab). To check hippocampal-dependent conditioning, mice were placed into the same training context and any tone or shock was presented.

To study fear extinction, the CFC training protocol was modified, as mice of different genotypes may acquire different levels of freezing behavior with the original paradigm. The new training protocol consisted of three consecutive electrical shocks (0.7 mA, 2-min intershock time), which resulted in similar freezing times for all mice. Extinction was studied for six consecutive days after training by placing animals (5 min) in the same context used for conditioning without the presence of a shock or tone.

Complementary Behavioral Test

Elevated-Plus Maze

We used an elevated plus maze to measure anxiety-like behavior. The maze is constructed by gray Plexiglas, elevated 50 cm above floor, and formed by a central platform (5 × 5 cm) from which arise two open and two closed arms (both 35 × 5 cm). The closed arms were surrounded by 15-cm high walls. Mice ($n=10$ per group) were placed in the central platform and freely allowed to explore the maze during 5 min.

Open Field Test

To assess spontaneous activity and response to a novel environment, we used the Open Field test. Mice ($n=10$ per group) were placed in 40 cm (length) × 30 cm (width) × 30 cm (height) dark plastic cages, and their behavior was recorded over 5 min. Using Ethovision XT software (Noldus), we analyzed the distance moved, the velocity of wandering and the time spent in both corners and center of the cage (Ares-Santos et al. 2014).

Novelty Suppressed Feeding Test

To assess the response to a novel environment, we used the NSFT (WT: $n=10$; *Drd2*^{-/-}: $n=8$). Before the test (24 h), animals were food deprived (with *ad libitum* access to water). During the test, animals were placed in a corner of a 40 cm (length) × 40 cm (width) × 30 cm (height) light plastic cage, with a regular pellet in the center of the arena. The mice were videotaped for 5 min, and the latency time to the first eat was recorded.

Porsolt Test

To assess motivation and susceptibility to negative mood, we used the Porsolt forced swimming test. This test was performed as previously described (Porsolt et al. 1978). Mice (WT: $n=10$; *Drd2*^{-/-}: $n=8$) were exposed to a single trial where they were forced to swim inside narrow Plexiglas cylinders (height, 25 cm; diameter, 10 cm) containing 10-cm water and maintained at 24–25 °C, and left there for 6 min. The total duration of immobility during the last 4 min of the trial was measured.

Rotarod

We used two different protocols to assess motor coordination and motor learning ($n=10$ per group). For motor coordination, mice were habituated for 10 min in the rod rotating at constant speed (4 rpm) and after 2 h, they were tested for 3 min at the same speed (Solis et al. 2015). For motor learning, we habituated the mice for 1 min at constant speed (4 rpm) and tested them in four consecutive trials of 5 min each (20 min apart) at constant acceleration (4–16 rpm). We measured the latency to first fall in both protocols, although if the mice fell, they were placed back in the rod.

Sensitivity to Electric Shock

This test was performed as described by Ortiz et al. (2010) to evaluate possible differences in sensitivity to an electric shock that may influence the behavioral responses. Briefly, mice ($n=10$ per group) were exposed to a consecutive foot-shocks that were incremented from low to mild-high intensities (0.02, 0.04, 0.06, 0.08, 0.1, 0.15, 0.2, 0.25, 0.3, 0.4, 0.5, 0.6 mA). Each foot-shock duration was a single second, with an intershock interval of 20 s. We recorded the shock intensity that resulted in the following initial sensation responses: sniffing and staring at the floor bars, licking, and biting the floor bars, alternating standing on paws, startling, jumping, and vocalizing.

Lentivirus

Lentivirus Construction (Lentiviral Plasmids)

To silence the mouse *Drd2* (GenID: 13489) in vivo and in vitro, three different sequences were designed and cloned into BamHI and XhoI sites of pRNAT-U6.2 by GenScript Corporation USA. The three siRNA used were: 5'-GAT CCC GCG TAG CAG CCG AGC TTT CTT CAA GAG AGA AAG CTC GGC TGC TAC GCT TTT TTC CAA CTC GAG-3' (*D₂RNAi01*), 5'-GGA TCC CGC GCC GAG TTA CTG TCA TGT TCA AGA GAC ATG ACA GTA ACT CGG CGC TTT TTT CCA ACT CGA G-3' (*D₂RNAi02*), and 5'-GGA TCC CGC TAC CTG ATA GTC AGC CTC TTC AAG AGA GAG GCT GAC TAT CAG GTA GTT TTT TCC AAC TCG AG-3' (*D₂RNAi03*). As a control, we used a mock siRNA with no target in mouse: 5'-GGA TCC CGA CGT CCA GGC TGC TTC GAT TGA TAT CCG TCG AAG CAG CCT GGA CGT CTT TTT TCC AAC TCG AG-3' (Control RNAi).

Lentivirus Production

Each lentiviral vector plasmid (pRNAT-U6.2-D2RNAi01, -i02, -i03; Genscript, USA) together with the packaging plasmid psPAX2 and the envelope plasmid pMD2G were co-transfected into HEK-293 T cells to produce viral particles. High-titer stocks (1×10^7 transduction units (TU)/ μL) were obtained by ultracentrifugation and resuspension of the viral pellet in PBS buffer. Viral stocks were stored at -80°C .

Determination of Lentivirus Silencing

The efficiency of the lentiviruses (Lv) at silencing was tested in vitro in the cell line *STHdh⁺/Hdh⁺* (CH00097; Coriell Institute) that overexpresses *Drd2*. These cells were grown at 33°C in a medium prepared with DMEM solution, 10% FBS (fetal bovine serum), 1% nonessential amino acids, 2 mM L-glutamine, 1% penicillin-streptomycin, 0.8 mg/mL geneticin, and 40 g/mL puromycin (Invitrogen). A total of 1×10^5 *STHdh⁺/Hdh⁺* cells were plated per well in 6-well plates. The next day, the cells were infected with 4 μL of each one of the three Lenti-*Drd2*-siRNA, or 4 μL of a mixture of the 3, or 4 μL of Lv-Mock-GFP (used as control). After 48 h, this medium was removed and replaced with fresh medium. After an additional 48 h, cells were solubilized in different lysis buffers for Western Blot (WB) or qRT-PCR.

For in vivo efficiency determination of lentiviral silencing, mice were stereotaxically injected in the striatum with 4 μL of the lentivirus particles mix ($n=4$) or siRNA control ($n=4$; 2 deposits of 2 μL each) using the coordinates: $DV_1 = -4$; $DV_2 = -3$; $AP = 0.65$; $L = \pm 2$ (see below for more stereotaxic surgery details). Four weeks after the surgery, mice were sacrificed by cervical dislocation and the striatum was dissected and fast frozen for analysis of protein and RNA.

Quantitative Real-Time PCR

RNA was extracted from the striatum or *STHdh⁺/Hdh⁺* cells using the illustra RNAspin kit (GE Healthcare) and retro-transcribed to cDNA. Quantitative PCR was carried out with SYBR Green dye (Applied Biosystems, USA) and oligonucleotides for *Drd2* and *Gapdh* (Forward: 5'-CAT TGT CTG GGT CCT GTT CCT-3'; 5'-ATG ACT CTA CCC ACG GCA AG-3'; Reverse 5'-GAC CAG CAG AGT GAC GAT GA-3'; 5'-CAT ACT CAG CAC CAG CAT CAC-3'). Triplicates were performed, and the values were standardized to amount of endogenous *Gapdh* mRNA content using the $\Delta\Delta\text{Ct}$ method (Granado et al. 2011).

Western Blotting

To check the silencing efficiency of Lv, we performed WB analyses with *STHdh⁺/Hdh⁺* lysates or striatum lysates as described previously (Ruiz-De Diego et al. 2014; Garcia-Sanz et al. 2017). We used primary antibodies for D_2R (1:1000, Millipore) and β -Actin (A5441, Sigma) followed by those for Horseradish Peroxidase (HRP, Vector) and detected the chemiluminescence with the ECL Substrate (BioRad). As loading control, we used β -actin or β -tubulin. A minimum of 3 experiments were performed for each study. Films were exposed and digitized signals were quantified with Quantity One software (BioRad).

Surgery

To carry out input/output curves, paired-pulse facilitation, LTP, and classical eyeblink conditioning, we used a set of four groups of mice: WT, *Drd2^{-/-}*, WT-GFP, and *Drd2*-siRNA ($n=10$ per group).

Mice injected with the siRNA particles were anesthetized with 0.8–1.5% isoflurane, supplied from a calibrated Fluotec 5 (Fluotec-Ohmeda) vaporizer, at a flow rate of 1–2 L/min oxygen (AstraZeneca) and delivered by a mouse anesthesia mask (David Kopf Instruments). In the first surgical step, animals from groups WT-Sham and *Drd2*-siRNA received a unilateral stereotaxic injection of 2 μL of Lv-Mock-GFP or a mix of Lv-*Drd2*-siRNAs of concentrated lentiviral stocks (0.2 $\mu\text{g}/\mu\text{L}$) into the hippocampus. The injection was carried out with a Hamilton syringe and performed unilaterally at the following coordinates, calculated from Bregma and skull surface: $AP = -2.4$; $L = +1.5$ (right side); $DV = -2.0$ (Franklin and Paxinos 2008).

Three weeks later, all animals included in the four groups mentioned above had bipolar stimulating electrodes implanted into the right side of the Schaffer collateral-commissural pathway of the dorsal hippocampus (2 mm lateral and 1.5 mm posterior to Bregma; depth of 1.0–1.5 mm from the brain surface; Franklin and Paxinos 2008) with a recording electrode in the ipsilateral stratum radiatum underneath the CA1 area (1.2 mm lateral and 2.2 mm posterior to Bregma; depth of 1.0–1.5 mm from the brain surface; Franklin and Paxinos 2008). The electrodes were made of 50- μm Teflon-coated tungsten wire (Advent Research Materials). The recording electrode was implanted in the CA1 area using the field potential depth profile evoked by paired (40-ms interval) pulses presented to the ipsilateral Schaffer collateral pathway. The recording electrode was fixed at the site where a reliable monosynaptic (≤ 5 ms) field excitatory postsynaptic potential (fEPSP) was recorded (Gruart et al. 2006, 2015). Evoked fEPSPs presented a large negative wave when the recording electrode was located at the stratum radiatum, and a positive shape when recorded near the pyramidal cell layer (Gruart et al. 2006, 2015). Animals selected for classical eyeblink conditioning were also implanted with stimulating electrodes on the left supraorbital nerve and recording electrodes in the ipsilateral orbicularis oculi muscle. Electrodes were made of 50- μm teflon-coated, annealed stainless steel wire (A-M Systems) bared at the tips for ~ 0.5 mm. The tips were bent into a hook to facilitate stable insertion in the upper eyelid. A 0.1-mm bare silver wire was affixed to the skull as a ground. All the wires were connected to 2 four-pin sockets (RS-Amidata). The sockets were fixed to the skull with the help of 2 small screws and dental cement. The implantation procedures used in this chronic preparation have been described in detail (Gruart et al. 2006, 2015). Experimental sessions started 1 week after surgery.

To verify the location of the stimulating and recording electrodes after completion of the experiments, mice were deeply re-anesthetized (sodium pentobarbital, 50 mg/kg), and perfused/fixated transcardially with saline and 4% phosphate-buffered paraformaldehyde (PFA). Selected brain sections (50- μm thick) including the dorsal hippocampus were obtained in a microtome (Leica), mounted on gelatinized glass slides, and Nissl stained with 0.1% toluidine blue.

Electrophysiology

Recordings were made using six differential amplifiers with a bandwidth of 0.1 Hz–10 kHz (P511, Grass-Telefactor; Fig. 1B). Hippocampal recordings were made with a high impedance probe ($2 \times 10^{12} \Omega$, 10 pF; Fig. 1B).

For input-output curves, the stimulus intensity was raised to 0.4 mA in steps of 20 μA . The selected interstimulus interval was 40 ms, because this results in maximum facilitation of the CA3-CA1 synapse (Madroñal et al. 2007). For paired-pulse

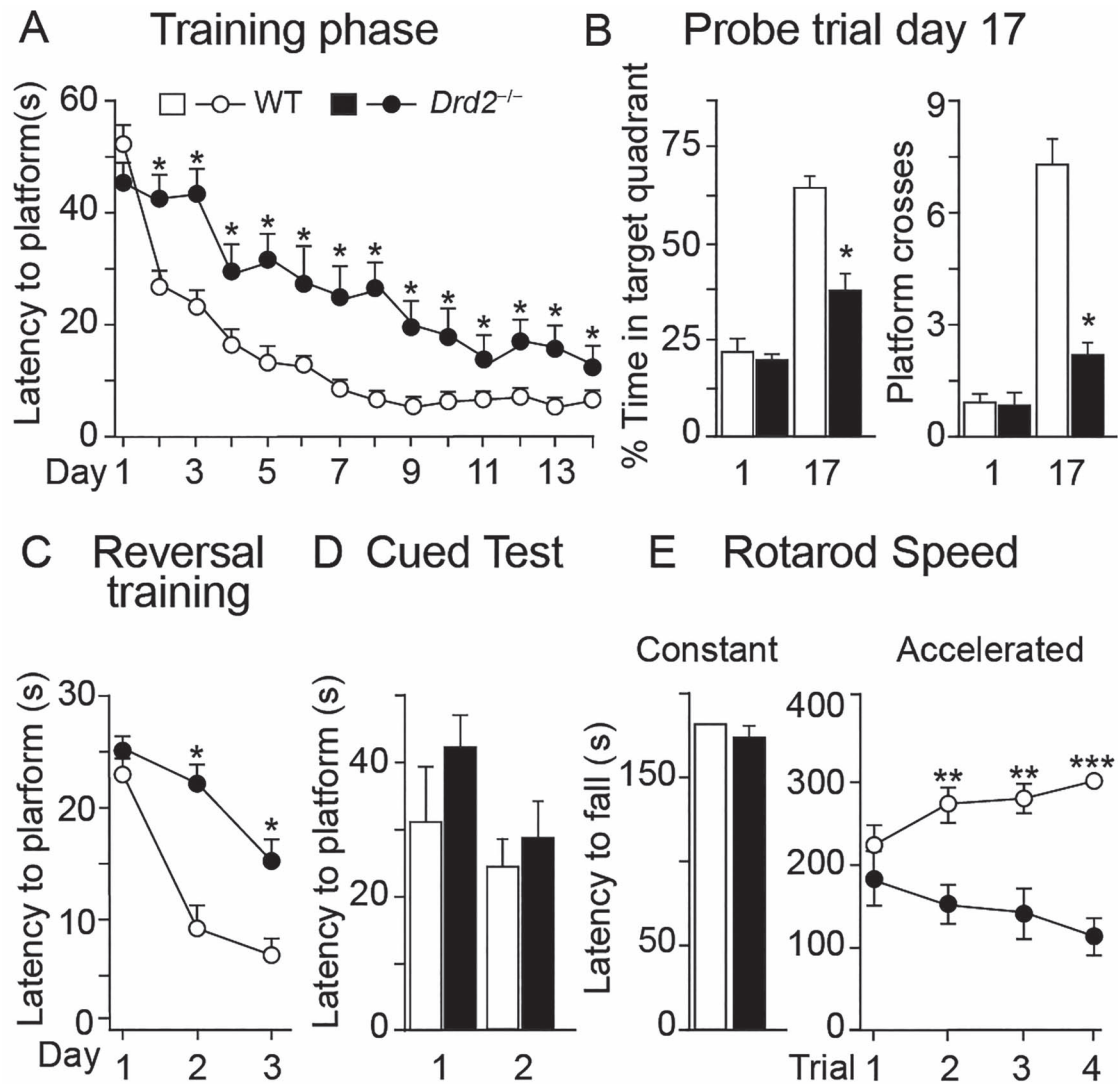


Figure 1. *Drd2* inactivation delays spatial learning in Morris Water Maze. (A) The reduction in latency during training occurred much more slowly in *Drd2*^{-/-} mice compared to their WT littermates ($P < 0.05$). (B) Probe trial performed 3 days after the training phase. Histograms represent the time spent searching in the target quadrant. *Drd2*^{-/-} mice increased their time in the target quadrant slightly compared to the first day of training; this increase was significantly lower than that seen in WT mice ($P < 0.001$). In the probe trial on day 17, *Drd2*^{-/-} mice made significantly fewer crosses through the platform location site than WT mice ($P = 0.006$). (C) Latency to find the platform during reversal phase. Here, we placed the platform opposite to the original place in the training phase. *Drd2*^{-/-} mice show an impaired reversal learning performance. ($P < 0.05$). (D) Cued version of MWM did not show differences between groups. (E) Rotarod at constant speed did not show differences. However, motor coordination learning in acceleration condition is impaired in *Drd2*^{-/-} mice ($P < 0.005$). Data show the mean values \pm SE. Repeated-measures two-way ANOVA followed by Tukey's test for post hoc analysis (A, D) and with Student's *t* test (B, C, E, F).

facilitation, pulse intensity (50–400 μ A) was set at 30%–40% of the level necessary to evoke an asymptotic fEPSP response, and the following interstimulus intervals were used: 10, 20, 40, 100, 200, and 500 ms (Gureviciene et al. 2004). In order to avoid unwanted interactions between successive pairs of stimuli, the interpulse delay was always ≥ 20 s.

For evoking LTP, we used a high-frequency stimulation (HFS) train consisting of 5 200 Hz, 100-ms trains of pulses at a rate of 1 pulse/s. This protocol was presented six times, at intervals of 1 min. As indicated above for paired-pulse facilitation, pulse intensity was set at 30%–40% of the level necessary to evoke a maximum fEPSP response for baseline recordings and after the HFS train. In order to avoid evoking a population spike and/or unwanted hippocampal seizures, the stimulus intensity during

the HFS train was set at the same intensity used for generating baseline records. Before presenting the animals with the HFS train, we collected baseline records for 15 min, using single pulses (a 100 μ s, square, negative–positive pulse) at a rate of 1 pulse/20 s. Following the HFS train, we presented the same set of pulses for 30 min. An additional recording session lasting 15 min was carried out 24 h after the HFS session (Gruart et al. 2006; Madroñal et al. 2016).

Classical Eyeblink Conditioning

Three animals at a time were placed in separate small (5 \times 5 \times 10 cm) plastic chambers located inside a larger (30 \times 30 \times 20 cm) Faraday box. Classical conditioning was

achieved using a trace paradigm consisting of a tone (20 ms, 2.4 kHz, 85 dB) presented as a CS. The US consisted of a cathodal, square pulse applied to the supraorbital nerve (500 μ s, $3 \times$ threshold) 500 ms after the end of the CS. A total of 2 habituation and 10 conditioning sessions were carried out for each animal. A conditioning session consisted of 60 CS-US presentations, and lasted ~ 30 min. For proper observation of conditioned response (CR) profiles, the CS was presented alone in 10% of the cases. CS-US presentations were separated at random by 30 ± 5 s. For habituation sessions, only the CS was presented, at the same frequency of 30 ± 5 s. As a criterion for CR, we consider the presence, during the CS-US interval, of electromyography (EMG) activity lasting >10 ms and initiated >50 ms after CS onset. In addition, the integrated EMG activity recorded during the CS-US interval had to be at least $2.5 \times$ greater than the averaged activity recorded immediately before CS presentation. The total number of CRs per session was computed and expressed as a percentage of the maximum (60 CRs per session = 100%).

Synaptic field potentials in the CA1 area were evoked during habituation and conditioning sessions by a single 100 μ s, square, biphasic (negative–positive) pulse applied to the ipsilateral Schaffer collaterals 300 ms after CS presentation. Stimulus intensities ranged from 50 to 250 μ A. For each animal, the stimulus intensity was selected according to data collected from the input–output curves, usually at $\sim 30\%$ of the intensity necessary for evoking a maximum fEPSP response (Gureviciene et al. 2004). An additional criterion for selecting stimulus intensity was that a second stimulus, presented 40 ms after a conditioning pulse, evoked a larger ($>20\%$) synaptic field potential (Gruart et al. 2006; Madroñal et al. 2016).

Immunofluorescence for GFP

Mice injected with lentivirus particles in CA1 were sacrificed and after that fixed using a solution of 4% of PFA in PBS overnight. Then, mice brains were sectioned at 30 μ m, using a vibratome, into coronal slices. On these slices, in a free-floating way, standard avidin-biotin immunohistochemistry was performed (Moratalla et al. 1996; Pavón et al. 2006; Granado et al. 2008; Espadas et al. 2012) with a rat antibody for GFP (1:1000, Nacalai Tesque Inc., Kyoto, Japan). Then, the tissue was incubated with reporter secondary antibody fluorescent Alexa green (488) antisera for 3 h (1: 500, Molecular Probes, Invitrogen, Eugene, OR, USA). Sections were mounted in a fluorescent mounting medium (DABCO, Fluka), coverslipped, and kept in the dark at 4 °C until they were examined by laser confocal microscopy (Leica).

Statistical Analysis

The SigmaPlot 12 program was used for all statistics and plotting. The threshold for statistical significance was set at $P < 0.05$.

Electrophysiology

With the help of an analog/digital converted (1410 Plus from CED), EMG and fEPSP recordings, and 1 V rectangular pulses indicative of CS and US presentations, were stored digitally on a computer with a resolution of 12 bits and at a sampling frequency of 11–22 Hz. Software (Spike 2 and SIGAVG; CED) was adapted to exhibit the selected electrophysiological (EMG and fEPSP) recordings. With the help of homemade programs, collected data were analyzed for the proper quantification of CRs

and fEPSP slopes (Gruart et al. 2006, 2015). Two-way ANOVA was used as statistic for analysis of the data, with group, session, or time as the repeated measure. When necessary and for further studies of significant procedures pairwise multiple comparison procedures (Holm–Sidak method) were added to determine additional significant differences. A regression analysis was carried out to determine the putative relationships between the percentage of CRs and fEPSP slopes.

Behavioral Values

Data are presented as mean \pm SE. To assess genotype and trial differences in MWM, active or passive avoidance, and CFC, repeated-measures two-way ANOVA was used with independent variables set as the genotype (WT and *Drd2a*^{-/-}) and time (short- and long-term memory tests in associative and special tasks). Post hoc comparisons with Tukey's test were performed for relevant differences. The quantification of the WB assay was analyzed using Student's *t* test.

Results

Dopamine D₂R is Important for Acquisition and Consolidation of Spatial Memory

Previous studies demonstrate an essential role of dopamine release in the dorsal hippocampus related to the acquisition and consolidation of spatial memory (Kempadoo et al. 2016). Dopamine D₂R_s are expressed in both the dorsal and ventral hippocampus, but are specifically enriched in the first one (Ishikawa et al. 1982; Wei et al. 2018). To assess the specific role of dopamine D₂R in spatial learning and memory, we used the spatial version of the MWM, a test known to require correct hippocampal function (Martin and Morris 2002; Granado et al. 2008; Ortiz et al. 2010). After habituation to the MWM, mice were given four training trials per day for 14 consecutive days. WT mice quickly learned to reach the platform, reaching the minimum escape latency by day 7, with no further change in escape latency between days 7 and 14 (Fig. 1A). In contrast, while escape latency on the first day of training was similar in *Drd2*^{-/-} and WT mice (Fig. 1A), the reduction in escape latency over the course of the training occurred more slowly in *Drd2*^{-/-} mice and showed significant differences from days 2 to 14 of training ($P < 0.05$) compared to WT. These results indicate that inactivation of *Drd2* does not completely inhibit learning, but significantly impairs it, so that extensive training is required to appropriately learn the task.

Retention was tested 3 days after the training period by removing the submerged platform (day 17). We measured the time that mice spent in each quadrant of the pool and the number of times they crossed through the platform location site. WT mice spent more time in the target quadrant ($64 \pm 3.6\%$) during retention testing than on the first day of training ($23.8 \pm 2.7\%$; Fig. 1B). Although *Drd2*^{-/-} mice slightly increased their time in the target quadrant compared to the first day of training, ($38.8 \pm 4.5\%$), this increase was significantly lower than that seen in WT animals (Fig. 1B, $P < 0.001$). Similarly, in the probe trial on day 17, *Drd2*^{-/-} mice made significantly fewer crosses through the platform location site than WT mice (2.2 ± 0.4 vs. 6.9 ± 0.8 ; $P = 0.006$; Fig. 1B). Taken together, these results indicate that consolidation of spatial memory is also impaired in the absence of D₂R.

Next, we analyzed the implications of *Drd2* for the acquisition of more complex spatial behaviors using a reversal test of the

Table 1 *Drd2*^{-/-} and WT mice show no differences in swimming speed (cm/s) in Morris Water Maze

Day	Swimming speed (cm/s)				
	1	4	7	10	14
WT	12.2 ± 1	13.3 ± 2	11.5 ± 1.5	13.3 ± 0.9	12.9 ± 0.7
<i>Drd2</i> ^{-/-}	11.8 ± 0.9	10.6 ± 1.7	10.3 ± 2	12.3 ± 1.2	12 ± 1.1

Notes: This table shows the swimming speed in Morris Water Maze (Fig. 1). No significant differences were found between the WT and *Drd2*^{-/-} mice

MWM. Correct coordination between the dorsal and ventral hippocampus and the medial prefrontal cortex is essential for the memory flexibility required for the reversal task (Avigan et al. 2020). Our results show that while WT mice were able to reduce the escape latency over three consecutive days from an average of 23.7 ± 2.52 s on day 1 to 7.8 ± 0.813 s on day three, the reduction was significantly smaller in *Drd2*^{-/-} mice: from 26.5 s on day 1 to 14.7 s on day 3 (Fig. 1C). WT animals needed just one training session to determine the new platform location, while *Drd2*^{-/-} mice needed more time to find the platform in the new location (Fig. 1C). This reduced learning is consistent with observations during acquisition and demonstrate an impairment in *Drd2*^{-/-} mice in the flexibility of memory required for the re-consolidation of new spatial tasks.

Locomotor Capability and Motivation of *Drd2*^{-/-} Mice

Previous studies have shown that *Drd2*^{-/-} mice have less spontaneous motor activity than their corresponding WT mice (Nakamura et al. 2014), which may lead to a reduced exploratory response. To verify that the apparent decrease in learning speed in *Drd2*^{-/-} mice is not simply the result of decreased locomotor activity, we measured swimming speed during the MWM training phase and found no significant difference in the average swimming speed on any of the training days (Table 1). In addition, no significant difference was observed between genotypes in the cued version of the MWM, a hippocampus-independent task traditionally used as a measure of motor capabilities and motivation (Fig. 1D), which indicates that the motivation to find the platform and exploratory behaviors of *Drd2*^{-/-} mice are similar to their WT littermates. Moreover, complex motor capabilities were tested using the Rotarod test. No differences between WT and *Drd2*^{-/-} mice were observed in motor coordination tested at constant speed, although clearly significant differences were observed at increasing speed, an index of motor learning ability (Fig. 1E).

These results indicate that our findings in the spatial learning assays cannot be attributed to abnormal motor behavior, decrease in exploratory behaviors, or motivational deficits, and support the conclusion that inactivation of *Drd2* delays spatial learning processes and markedly impairs memory consolidation.

Associative Learning and Memory are Impaired in *Drd2*^{-/-} Mice

Strong evidence supports the important role that dopamine plays in associative learning and memory tasks (Groessi et al. 2018; Handler et al. 2019; Iino et al. 2020). In addition, recent studies indicate that D₂Rs may play an essential role in aversive behaviors through detecting and regulating changes in dopamine signals that are induced in these trainings (Danjo et al. 2014; Iino et al. 2020). However, there is still no evidence of

whether and how this receptor can differentially influence each particular phase of acquisition, consolidation and extinction, and the impact of its absence.

To assess this, we used passive avoidance, an associative task that depends on the correct coordination of different brain areas including the hippocampus, cortex, striatum and amygdala. Notably, passive avoidance learning requires dopamine signaling in the striatum and the amygdala (Darvas et al. 2011) and D₁R plays a significant role in this behavior (Ortiz et al. 2010). To study the role of D₂R, we first determined the sensitivity to electric foot-shock in WT and *Drd2*^{-/-} mice by gradually increasing the intensity (0.01–0.6 mA) and recording the threshold for staring at bars, startle response, and jumping and vocalization, indicators of increasing pain sensation (Fig. 2A). WT and *Drd2*^{-/-} mice showed similar thresholds for all three behavioral signs: approximately 0.05 mA for staring at bars, 0.1 mA for the startle response, and 0.17 mA for jumping (Fig. 2A), indicating that there is no difference in the sensitivity of *Drd2*^{-/-} mice compared to WT, agreeing with previous studies that showed no differences in nociception between these genotypes (Mansikka et al. 2005).

Passive avoidance results show that basal entry latency times were similar in all experimental groups. WT and *Drd2*^{-/-} mice increased their latency times at 1 and 24 h after the foot-shock. However, 1 h after the stimulus, the increase in latency was significantly smaller in *Drd2*^{-/-} mice than in WT mice ($P < 0.05$; Fig. 2B), indicating a deficit in the acquisition or short-term memory retention of *Drd2*^{-/-} mice. No difference was observed at 24 h, suggesting that both groups of mice are able to consolidate the learning. These differences suggest a deficit in the acquisition, but not in the long-term consolidation of passive avoidance due to *Drd2* inactivation.

In contrast, in the two-way active avoidance task, *Drd2*^{-/-} mice were completely unable to learn, in agreement with a study showing that a partial deletion of *Drd2* (*Drd2L*^{-/-}) induced a significant impairment in the acquisition of avoidance responses in the 2-way active avoidance, similar to aged WT mice (Fetsko et al. 2005). While WT mice learned the task during the first 3 days, there was no change in the response of the *Drd2*^{-/-} mice throughout the entire training phase (11 days). Indeed, *Drd2*^{-/-} mice only cross to the other compartment after the electric shock, in almost all the trials (escape responses). These results indicate that *Drd2*^{-/-} mice did not learn to associate the CS with the foot-shock (Fig. 2C,D, $P < 0.001$, 2-way ANOVA). In fact, *Drd2*^{-/-} mice crossed to the other compartment only when the shock was delivered within 5 s of starting the trial (Fig. 2E). Inter-trial interval crosses were slightly higher, but not significantly, in *Drd2*^{-/-} compared with WT mice for the first 3 days (Fig. 2F), supporting the conclusion that the poor performance of *Drd2*^{-/-} mice in this paradigm is due to impaired associative learning and not to lower locomotor activity.

Differences in the execution of both passive and active avoidance indicate the different role of D₂R in the distinctive pathways involved in these 2 forms of associated learning.

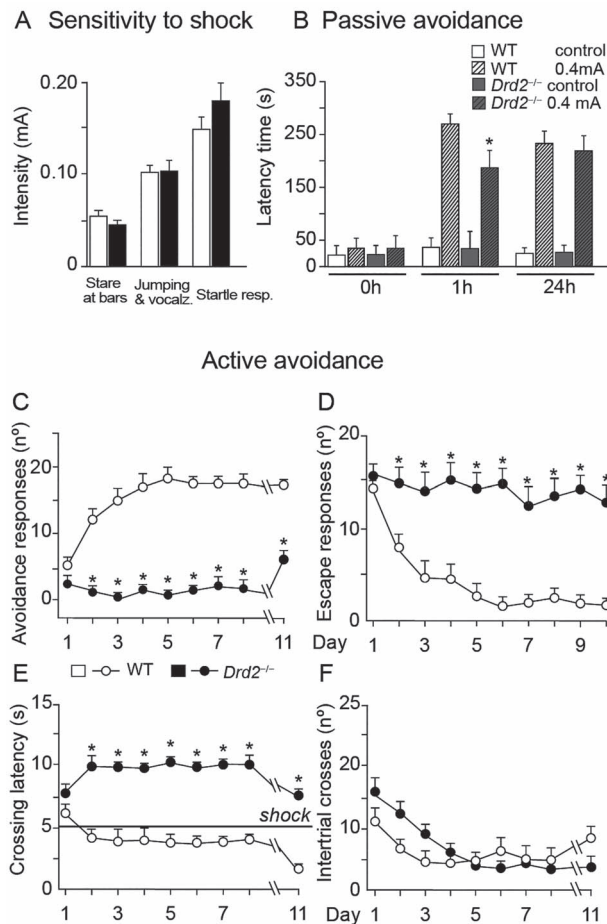


Figure 2. *Drd2*^{-/-} mice showed critically impaired associative avoidance responses. (A) Threshold responses to increasing intensity foot-shocks were similar in both genotypes ($n = 10$ mice per group). (B) Passive avoidance latency refers to the time spent in the light compartment, which was paired with foot-shock in a single training trial. WT and *Drd2*^{-/-} mice increased their latency times at 1 and 24 h after the foot-shock. However, 1 h after the stimulus, the increase in latency was significantly ($P < 0.05$) smaller in *Drd2*^{-/-} mice than in WT mice. No difference was observed at 24 h. (C) Progression of avoidance responses during the training phase. WT mice quickly learn to avoid the shock while *Drd2*^{-/-} mice did not learn to avoid it during the entire 11-day training phase, indicating that these mice did not learn to associate the CS with the foot-shock ($P < 0.001$). (D) Number of escape responses during the training days. *Drd2*^{-/-} mice shown more escape responses during the entire training phase, indicating they respond almost only when the shock is delivered ($P < 0.001$). (E) Time course of crossing latencies during the training phase. $P < 0.001$ versus WT mice. (F) Number of inter-trial crosses. The number of inter-trial crosses was similar in both genotypes, indicating that *Drd2*^{-/-} mice have the same crossing ability as WT. Data show the mean values \pm SE. Statistics were determined by repeated-measures two-way ANOVA followed by post hoc analysis with Tukey's test. WT ($n = 10$) and *Drd2*^{-/-} ($n = 10$).

Drd2^{-/-} mice behavior in active avoidance suggests a robust impairment in the acquisition that caused a possible learning helplessness phenomenon. For this reason, and due to the essential role of dopamine in motivational and emotional features, we decided to evaluate the emotional responses of *Drd2*^{-/-} mice to find possible differences in this phenotype compared to WT group. First, we evaluated the general activity of *Drd2*^{-/-} mice in the open field. *Drd2*^{-/-} mice showed significantly less distance traveled and at lower velocity

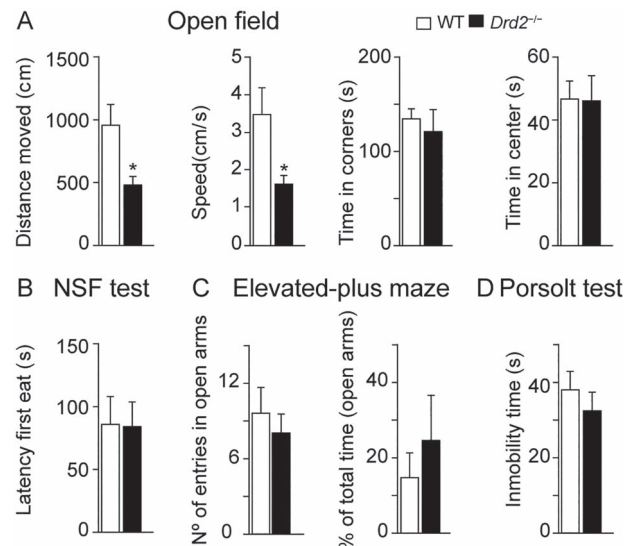


Figure 3. *Drd2* inactivation does not affect emotional or motivational responses. (A) Open field results shown significant differences between groups in distance (cm) and velocity (cm/s; $P < 0.005$) whereas time in corner and center did not differ between genotypes. (B) NSF. Latency values to the first eat were similar between *Drd2*^{-/-} and WT mice. (C) Elevated-plus maze: anxiety-like behavior of *Drd2*^{-/-} and WT mice is illustrated by the number of entries and percentage of total time spent in the open arms of the elevated-plus maze. *Drd2*^{-/-} mice showed similar number of entries and time spent in the open arms. (D) Porsolt: WT and *Drd2*^{-/-} mice showed similar immobility time. Data shown are mean \pm SE. Statistical values were determined by Student's *t* test.

than their WT littermates (Fig. 3A, $P < 0.005$), unlike with the swimming speed we found in MWM (Table 1) or in the intertrial crossings number (two-way active avoidance, Fig. 2F). However, the time spent in the corners and in the center of the field was similar between both genotypes (Fig. 3A). These results suggest a hypokinesia at the basal level of *Drd2*^{-/-} mice that may not affect the spontaneous exploratory responses or other motivational or emotional disturbances.

To verify this hypothesis, we performed a battery of experiments to specifically evaluate motivational and emotional aspects of *Drd2*^{-/-} mice that may also explain the pattern of response observed in active avoidance tasks. These tests were as follows: the novelty suppressed feeding test that showed similar latency to the first eat for the 2 groups (Fig. 3B), the elevated-plus maze that showed no significant differences in the number of entries or the percentage of time spent in the open arms (Fig. 3C) and the Porsolt test with similar immobility times for both groups (Fig. 3D). Taken together, these results indicate that the pattern of response observed in *Drd2*^{-/-} mice group in active avoidance is not a consequence of an abnormal emotional or motivational response associated to their phenotype. This pattern of response is likely due to a critical and specific deficit in associative learning as well as its long-term consolidation.

Finally, to clarify the role of D₂R in hippocampal-dependent associative memories, we used the contextual fear conditioning task that measures the ability to associate an aversive stimulus, in this case an electric foot-shock (US), with a neutral environmental context (CS). In this test, we evaluated the percentage of time that the animals froze when re-exposed to the CS. In our experiments, baseline levels of freezing were similar in the two genotypes before the shock (Fig. 4A). However, immediately after the shock, *Drd2*^{-/-} mice spent significantly ($P < 0.01$) less

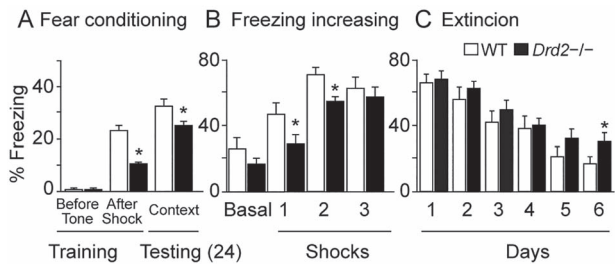


Figure 4. *Drd2* inactivation reduces fear conditioning but does not alter fear extinction. (A) After the shock, *Drd2*^{-/-} mice spent significantly ($P < 0.01$) less time freezing than their WT littermates, and 24 h after shock, freezing times were still significantly lower in *Drd2*^{-/-} mice, although the magnitude of the difference was reduced ($P < 0.01$). (B) Freezing time after 3 foot-shocks separated by 2 min to reach similar freezing times in both genotypes. (C) Daily freezing time in the context without foot-shock. The extinction curve was similar for both groups of mice, except on the last day, when *Drd2*^{-/-} mice had higher values indicating lower extinction. Data shown are mean \pm SE. Statistics were performed with repeated-measures 2-way ANOVA, followed by post hoc analysis with Tukey's test.

time freezing than their WT littermates, and 24 h after the shock, freezing times were still significantly lower in *Drd2*^{-/-} mice, although the magnitude of the difference was reduced (Fig. 4A). These results suggest that both acquisition and consolidation of hippocampal-dependent associative memories are impaired in *Drd2*^{-/-} mice.

To study fear extinction, 48 h after fear conditioning, we delivered three consecutive foot-shocks separated by 2 min to establish similar freezing times in both genotypes (Fig. 4B), as described previously (Ortiz et al. 2010). Subsequently, mice were tested daily for freezing in the US context for six consecutive days without foot-shock. The extinction curve was similar for both groups of mice, with *Drd2*^{-/-} mice presenting slightly higher values every day. However, these differences were not significant when analyzed along the extinction trials by a 2-way mixed ANOVA test ($F_{5,132} = 0.33$; $P > 0.05$), indicating no statistically significant differences between *Drd2*^{-/-} and WT mice in the extinction of conditioned fear responses.

Knockdown of Dopamine D₂R In Vitro and In Vivo Experiments

Despite of the consistent results obtained with our *Drd2*^{-/-} mice, the constitutive deletion of an important receptor such as the D₂R may have developmental compensatory mechanisms altering behavioral responses. Additionally, the complete absence of D₂R in other brain areas can also affect these responses including hippocampal-dependent tasks. For this reason, we decided to specifically knock-down dopamine D₂R expression in the hippocampus of adult animals using Lv-based RNA interference. We designed three siRNAs that targeted different regions of the *Drd2* mRNA and inserted each siRNA into the transfer plasmid. The efficiency of *Drd2* silencing was assessed in *STHdh*⁺/*Hdh*⁺ cells (Fig. 5A). Four days after the infection, there was a dramatic decrease in D₂R protein expression in these cells with the Lv-*Drd2*-siRNA mix compared with the cells given Lv-GFP.

We also assess the in vivo silence capacity of Lv-*Drd2*-siRNAs lentiviral particles in the striatum because D₂R expression in this region is higher than in the hippocampus. We stereotaxically injected 4 μ L of the Lv-*Drd2*-siRNAs mix or Lv-Mock-GFP as a control in the striatum of mice. One week after the injection, there were intense and significant decreases in mRNA levels

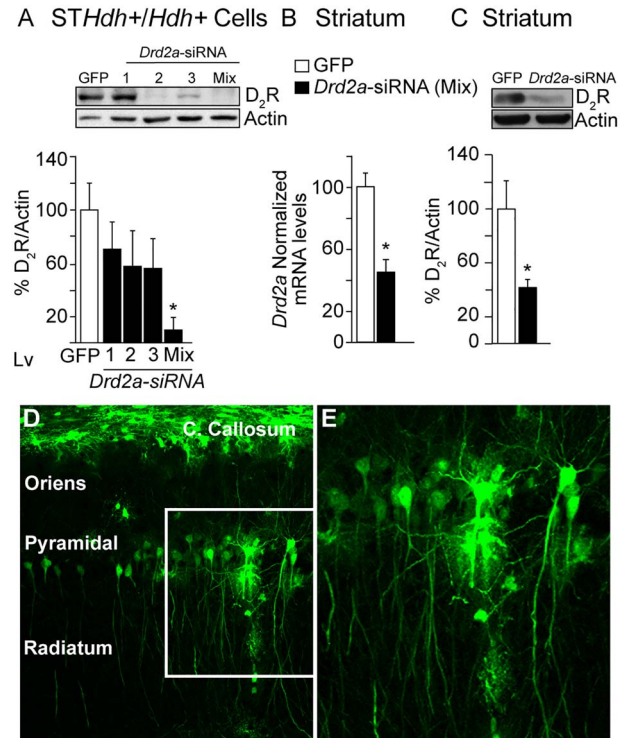


Figure 5. Efficient in vitro and in vivo silencing of *Drd2* by siRNA. (A) Drastic reduction of *Drd2* protein expression in *STHdh*⁺/*Hdh*⁺ cells in vitro after infection with *Drd2*-siRNA constructs ($P = 0.014$). (B) *Drd2* mRNA levels in striatum 48 h after injection of *Drd2*-siRNAs mixture. mRNA levels were determined by RT-PCR, normalized to Actin, and expressed as a percentage of *Drd2* mRNA expression in Lv-GFP-injected animals. Injection of *Drd2*-siRNAs specifically decreased *Drd2* mRNA expression. (C) D₂R protein levels were decreased 48 h after injection of siRNAs. D₂R protein levels were decreased after injection of siRNAs $P = 0.0049$, and levels in *Drd2*^{-/-} mice were $P = 0.021$, Student's *t* test. (D) Photomicrograph of a coronal brain section that shows the lentiviral infection in the CA1 layer of the hippocampus of WT mice after injection with lenti-GFP particles (2 μ L). (E) Highly magnified image of the infected pyramidal cells from panels D, E. Particles have infected a large portion of the dorsal hippocampus, and are spreading through the pyramidal CA1 cell layer. Scale bar: 100 μ m.

(Fig. 5B) and D₂R protein (Fig. 5C) in *Drd2*-siRNA-injected mice compared with animals given injections of Lv-GFP.

After verifying the efficiency of the lentiviral particles in the striatum, a new set of animals were bilaterally infused (2 μ L) in the hippocampus to evaluate the viral diffusion in this area. We used immunohistochemistry to determine how far the virus had spread into the hippocampus in the Lv-GFP-injected mice. Our results show that particles infected most of the dorsal hippocampus, reaching ~ 2 mm² along the rostrocaudal axis (Fig. 5D,E).

Input/Output Curves and Paired-Pulse Facilitation in the CA3-CA1 Synapse were Normal in *Drd2*^{-/-} and in *Drd2*-siRNA Mice

As already indicated in the Methods section, to determine the basal synaptic transmission in the four groups of alert behaving mice (WT, *Drd2*^{-/-}, WT mice injected with Lv-*Drd2*^{-/-} siRNA [*Drd2*-siRNA] and WT-Sham mice), we measured fEPSPs evoked at the CA3-CA1 synapse by the electrical stimulation of Schaffer collaterals at increasing intensities (0.02–0.4 mA, in 0.02 mA steps). Input-output curves revealed no significant differences

in basal synaptic transmission between the four groups (Fig. 6A). Interestingly, input–output curves collected from the four groups of mice ($n=10$ animals/group) were best adjusted by similar sigmoid curves ($r \geq 0.984$; $P < 0.001$). Using the double-pulse test with interpulse intervals ranging from 10 to 500 ms, we found a significant ($F_{5,45} = 50.45$; $P < 0.001$) increase in the slope of fEPSPs evoked by the second pulse at short time intervals (10–100 ms). There were no significant differences between WT, *Drd2*^{-/-}, WT-Sham, and *Drd2*-siRNA mice ($F_{15,45} = 1.42$; $P = 0.181$, Fig. 6B).

LTP Evoked at the CA3-CA1 Synapse is Decreased in Behaving *Drd2*^{-/-} and in *Drd2*-siRNA Mice

To determine the relevance of hippocampal D₂Rs in LTP, we recorded and quantified CA3-CA1 fEPSPs following HFS of Schaffer collaterals in WT, *Drd2*^{-/-}, WT-Sham, and *Drd2*-siRNA mice ($n=10$ animals/group; Fig. 6C,D). To determine baseline responses, Schaffer collaterals were stimulated every 20 s for 15 min. The stimulus consisted of a 100- μ s, square, negative–positive pulse. After HFS, the same single stimulus was presented every 20 s for 30 min and repeated 24 h later for 15 min. We found LTP in WT and WT-Sham mice for the two recording sessions (Fig. 6C,D). As already reported for the hippocampal CA3-CA1 synapse (Gruart et al. 2006, 2015; Madroñal et al. 2007, 2016; Ortiz et al. 2010), 15 min after HFS, the response to the single stimulus in both WT ($F_{11,99} = 60.38$) and WT-Sham ($F_{11,99} = 15.15$) groups was >150% of baseline values ($P < 0.001$; white circles, Fig. 6C,D). Significant LTP persisted at 24 h post-HFS ($P < 0.001$; Fig. 6C,D). Although *Drd2*^{-/-} mice showed a small (<150%) LTP at the CA3-CA1 synapse after HFS (Fig. 6C, black circles), the collected fEPSP slopes were significantly smaller ($F_{11,99} = 20.71$; $P < 0.001$) than values collected from WT animals for the two post-HFS sessions. Slopes of fEPSP collected from *Drd2*-siRNA mice after the HFS (Fig. 6D, black circles) were significantly ($F_{11,99} = 2.464$; $P < 0.01$) smaller than those collected from WT-Sham only during the second post-HFS session. Thus, both *Drd2*^{-/-} and *Drd2*-siRNA mice presented a reduced LTP in the hippocampal CA3-CA1 when compared with their littermate controls.

Classical Trace Eyeblick Conditioning is Significantly Reduced in *Drd2*^{-/-} and *Drd2*-siRNA Mice

As already reported in previous studies, classical eyeblink conditioning is a hippocampal-dependent type of associative learning, mainly when using a trace paradigm as reported here (Thompson 1988; Gruart et al. 2006). In addition, we have also showed that the synaptic activity at hippocampal synapses is modulated during the acquisition of trace conditioning tasks (Gruart et al. 2006; Ortiz et al. 2010). In Fig. 7A,B, we illustrate that the neural premotor circuits involved in the generation of reflex eyelid responses function normally in the four groups of animals. Reflex eyeblinks evoked by the electrical stimulation of the supraorbital nerve were similar to previous descriptions in WT mice (Gruart et al. 2006). There were no significant differences between the four groups of mice in the latency and amplitude of reflexively evoked blinks (not illustrated; $P \leq 0.362$).

To investigate the behavioral consequences of the synaptic plasticity deficit in the CA3-CA1 synapse observed in *Drd2*^{-/-} and *Drd2*-siRNA mice, we evaluated classical conditioning of eyeblink responses in the four groups ($n=10$ animals/group). We used a trace paradigm (CS, tone; US, shock) with a 500-ms interval between the end of the CS and the beginning of the US (Fig. 7A,B). As illustrated in Fig. 7C, WT mice increased the

percentage of CRs across the successive conditioning sessions, being significantly different from habituation values from the third to the tenth conditioning sessions ($F_{11,99} = 81.67$; $P < 0.001$; Fig. 7C). This learning curve presented a profile similar to that reported previously in WT mice (Takatsuki et al. 2003; Gruart et al. 2006; Ortiz et al. 2010). In contrast, the percentage of CRs in the *Drd2*^{-/-} group increased more slowly, reaching lower asymptotic values than their littermate controls (Fig. 7C). Thus, the percentage of CRs presented by the WT group was significantly different from that of the *Drd2*^{-/-} group from the fourth to the tenth conditioning sessions ($F_{11,99} = 2.013$; asterisks in Fig. 7C; $P = 0.035$). Similarly, WT-Sham animals presented learning curves ($F_{11,99} = 46.256$; $P < 0.001$) similar to those seen in WT mice, while CRs in *Drd2*-siRNA mice presented a significantly lower percentage of CRs from the sixth to the tenth conditioning sessions ($F_{11,99} = 2.532$; $P = 0.007$; asterisks in Fig. 7D).

Learning-dependent Changes in CA3-CA1 Synaptic Strength were Reduced in *Drd2*^{-/-} and *Drd2*-siRNA Mice

As shown in behaving mice, trace eyeblink conditioning is associated with an increase in synaptic strength at the hippocampal CA3-CA1 synapse (Gruart et al. 2006, 2015; Madroñal et al. 2007, 2016). We evaluated the effect of D₂R loss on fEPSPs evoked at the CA3-CA1 synapse. Electrical stimulation of Schaffer collaterals 300 ms after CS presentation evoked an fEPSP in the CA1 area in all four experimental groups (Fig. 7A,B). Although the stimuli presented to Schaffer collaterals disrupted the regular theta rhythm recorded in the CA1 area, the rhythm reappeared in phase about 200 ms afterwards. The slope of the evoked fEPSPs increased in the four experimental groups over the course of conditioning when Schaffer collateral stimulation took place during the CS-US interval (Fig. 7E,F).

Nevertheless, there were clear differences between the two controls (WT and WT-Sham) and the two experimental (*Drd2*^{-/-} and *Drd2*-siRNA) groups ($n=10$ animals/group). In agreement with previous studies (Gruart et al. 2006, 2015; Madroñal et al. 2007, 2016; Ortiz et al. 2010), and as illustrated in Figure 7E,F, fEPSP slopes recorded in WT (140%; $F_{11,99} = 22.730$; $P < 0.001$) and WT-Sham (120%; $F_{11,99} = 14.585$; $P < 0.001$) mice were significantly elevated over baseline values by the tenth conditioning session. In contrast, although the slopes of evoked fEPSPs in *Drd2*^{-/-} (120%; $F_{11,99} = 22.730$; $P < 0.001$) and *Drd2*-siRNA (110%), mice were elevated over baseline, they were smaller than in the corresponding control animals (Fig. 7E,F). Collected fEPSP slopes were significantly different between WT and *Drd2*^{-/-} mice (asterisks in Fig. 7E; $F_{11,99} = 1.614$; $P < 0.05$), but not between WT-Sham and *Drd2*-siRNA animals ($F_{11,99} = 1.473$; $P = 0.154$). In summary, the decreased performance in associative learning tasks noticed in *Drd2*^{-/-} and *Drd2*-siRNA mice compared with their respective controls was paralleled by a decline in activity-dependent increases in synaptic strength at the CA3-CA1 synapse during classical conditioning of eyelid responses.

Discussion

We analyzed the role of D₂R in memory and the synaptic plasticity processes. Genetic inactivation of D₂R in mice significantly impairs their ability to perform spatial and associative acquisition and memory consolidation. In addition, D₂R constitutive deletion or partial inactivation in the CA1 hippocampal region significantly impaired associative learning, LTP and classical trace eyeblink conditioning.

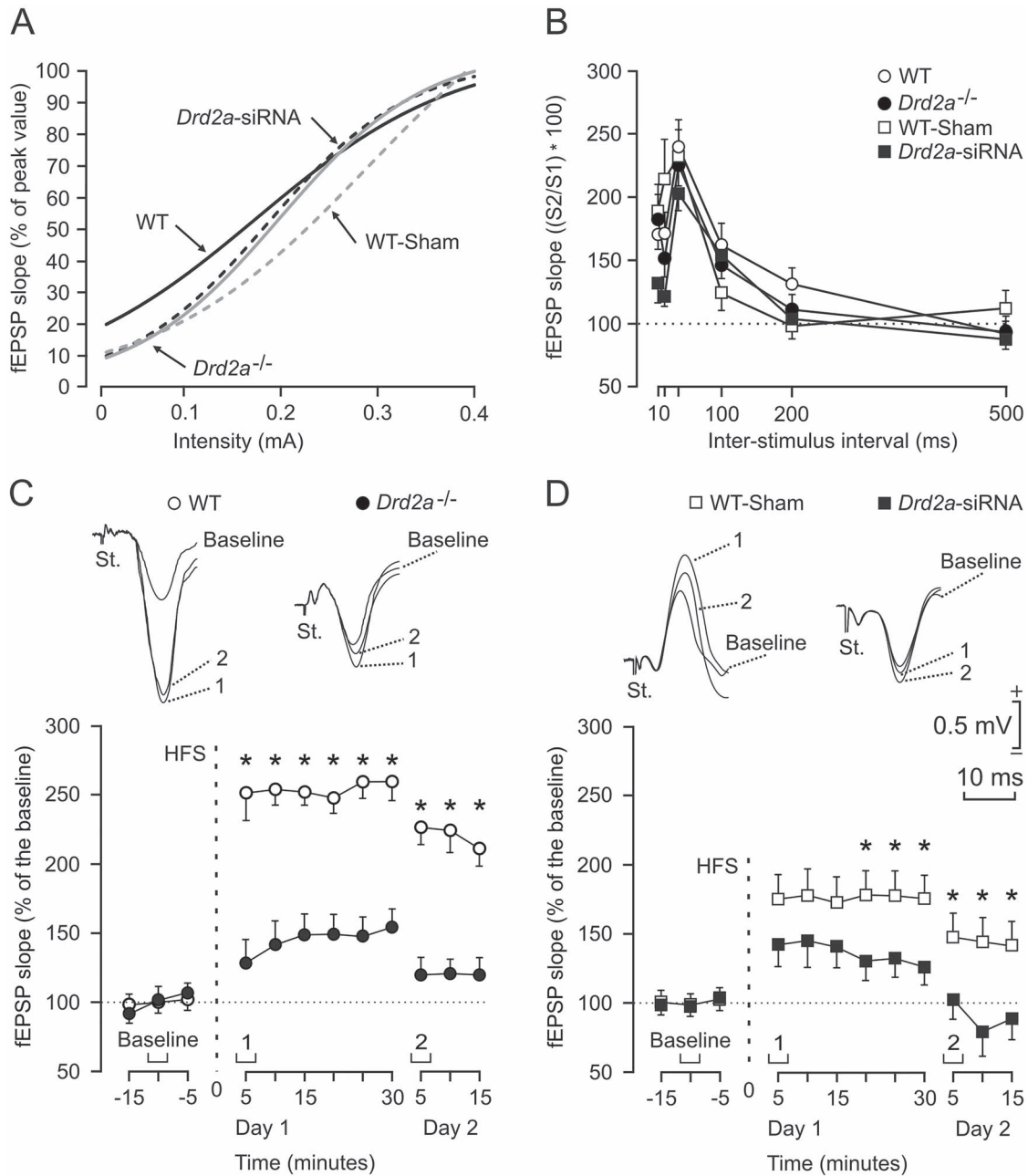


Figure 6. LTP evoked at the CA3-CA1 synapse is decreased in behaving *Drd2*^{-/-} and in *Drd2*-siRNA mice. (A) Input-output curves collected from the 4 experimental groups. Stimulus consisted of single pulses presented at increasing intensities in 20 μ A steps. Collected data was best adjusted by sigmoid curves ($r \geq 0.984$; $*P < 0.001$; $n = 3$ animals per group), with no significant ($P = 0.067$) differences between groups. (B) Paired-pulse facilitation of fEPSPs recorded in the CA1 area following stimulation of Schaffer collaterals. The data shown are mean \pm SE slopes of the second fEPSP expressed as a percentage of the first of the six (10, 20, 40, 100, 200, and 500 ms) interpulse intervals. The four groups of mice presented a significant ($*P < 0.05$) paired-pulse facilitation at short (10–40 ms) interpulse intervals, but no significant differences ($P = 0.181$) between groups. (C) At the top are illustrated representative fEPSPs recorded from WT and *Drd2*^{-/-} animals before (baseline), and 5 min (1) and 24 h (2) after HFS. Graphs illustrate the time course of changes in fEPSPs (mean \pm SE) following HFS stimulation of the Schaffer collaterals. The HFS train was presented after 15 min of baseline recordings, at the time marked by the dashed line. fEPSPs are given as a percentage of the baseline (100%) slope. WT mice (white circles) presented a significantly larger LTP than *Drd2*^{-/-} (black circles) animals ($*P < 0.001$). (D) Same analysis as in C for WT-Sham and *Drd2*-siRNA groups. Here again, the control group presented a significantly larger LTP than *Drd2*-siRNA mice ($*P < 0.05$).

Drd2^{-/-} Mice Exhibit Impaired Spatial Memory

Previous studies found that DD-mice (Darvas and Palmiter 2009) and *Drd1a*^{-/-} mice (Granado et al. 2008; Ortiz et al. 2010; King et al. 2010) show impaired spatial memory. To understand how D₂R determines spatial learning and memory, we used the

hippocampal-dependent task MWM (Martin and Morris 2002). We found that *Drd2*^{-/-} mice showed significantly impaired acquisition, consolidation, and reversal learning in agreement with previous studies showing that pharmacological blockade or genetic D₂R deletion impair spatially related memory task

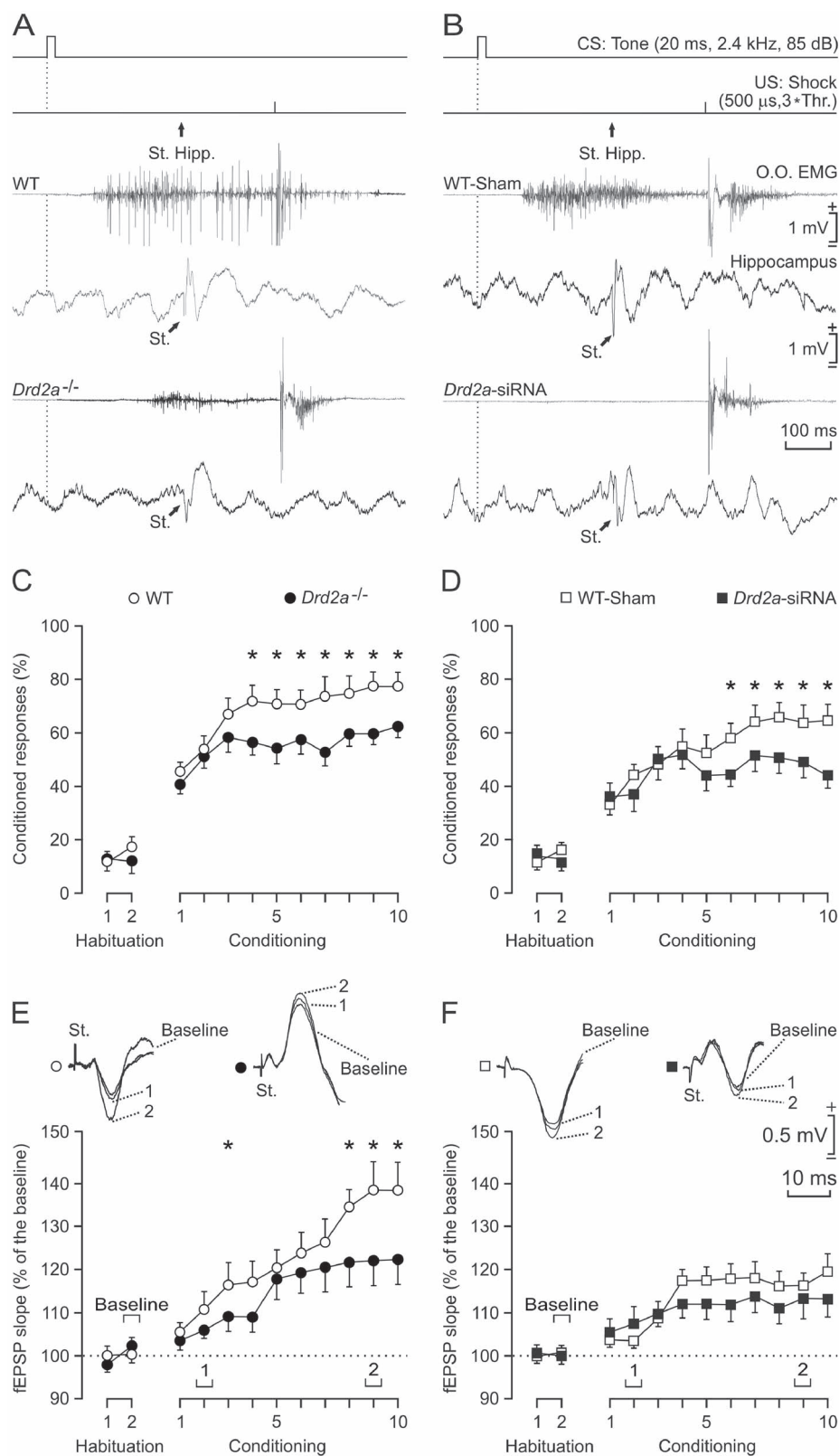


Figure 7. Learning-dependent changes in CA3-CA1 synaptic strength are impaired in *Drd2*^{-/-} and *Drd2*-siRNA mice. (A, B) From top to bottom are illustrated the conditioning paradigm, representative EMG and hippocampal recordings collected during paired CS-US presentations for WT and *Drd2*^{-/-} mice (A) and for WT-Sham and *Drd2*-siRNA mice (B). The moment of stimulus presentation at Schaffer collaterals (St.) is indicated, as is the time of delivery of CS (dashed line). Data shown were collected during the ninth conditioning session. (C, D) Percentage of eyelid CRs reached by the four experimental groups. The acquisition curve presented by the WT (white circles) group was significantly larger than values reached by the *Drd2*^{-/-} (black circles) group (C; **P* < 0.05). The acquisition curve of the WT-Sham

performance (Rocchetti et al. 2015). However, others found that D₂R antagonists could improve the performance in MWM (Setlow and McGaugh 1999, 2000). Here, D₂R antagonist was given at the end of the training, affecting the memory consolidation process, but not the acquisition that we demonstrated is also impaired. In addition, this can be also attributed to the poor specificity of the D₂R pharmacological agents. Models based on genetic inactivation like ours provide a more reliable approach toward a better understanding of the D₂R specific function.

On the other side, several previous studies indicate that D₂R is essential for motor responses (Kravitz et al. 2010; Beeler et al. 2016; Bamford et al. 2018; Solis et al. 2019). Our results show that complex motor coordination responses, such as those required in the accelerated rotarod, are impaired by D₂R genetic deletion. However, motor coordination in constant speed in the Rotarod, or swimming speed in the MWM, and the number of intertrial crossings in the active avoidance test were similar between genotypes, perhaps because these behaviors do not require complex motor programs. For these reasons, we consider that the motor deficits cannot completely explain the impairment observed in spatial and associative learning and in the memory test, although with the constitutive *Drd2*^{-/-} mice, we cannot rule out this possibility.

Another relevant aspect to point out is the particular role of D₂Rs in motivated behaviors. D₂R-expressing neurons, especially in the striatum and nucleus accumbens, are critically involved in motivation (Soares-Cunha et al. 2016; Olivetti et al. 2020). However, our *Drd2*^{-/-} mice did not show motivational differences in cued test and NSF compared to their WT littermates, but this could also represent a limitation of the use of full *Drd2*^{-/-} mice.

Associative Learning is Impaired in *Drd2*^{-/-} Mice

To assess the role of D₂R in associative learning, we used three paradigms to evaluate hippocampal-dependent fear memories. In passive avoidance acquisition test (1 h), *Drd2*^{-/-} animals showed significant impairment, but not 24 h after training, compared to WT mice. This indicates that the impairment associated with D₂R deletion is due to abnormal acquisition of inhibitory learning or short-term memory retrieval, and less from long-term consolidation in passive avoidance. In this line, previous studies found that presynaptic D₂R is involved in acquisition of inhibitory responses and reversal learning in operant tasks (Linden et al. 2018).

Additionally, *Drd2*^{-/-} mice showed less freezing after CFC training and in the long-term retention (24 h), suggesting a poor hippocampal consolidation of the fear memory associated to context, similar to DD-mice (Fadok et al. 2009). In addition, WT and *Drd2*^{-/-} mice showed a delay in the freezing extinction, only significant in the final day. A recent study showed that striatal D₂Rs are not required for the extinction (Iino et al. 2020). However, another recent study indicated that striatal D₂Rs may control the updating of a learning process and affect the flexibility required in goal-directed behaviors altering extinction (Matamales et al. 2020). This controversy can be explained

by the recent characterization of D₂Rs striatal subpopulations through the dorso-ventral axis (Puighermanal et al. 2020). Specific populations of D₂R-expressing neurons in the striatum may develop highly specialized functions modulating precise aspects of cognition.

Finally, we demonstrated that *Drd2*^{-/-} mice display similar deficits to *Drd1a*^{-/-} mice in active avoidance (Ortiz et al. 2010). *Drd2*^{-/-} animals did not have decreased escape latency and displayed a response pattern similar to that observed in models of “learned helplessness” (Seligman et al. 1975). This type of response can be explained by an increase in the stress vulnerability of *Drd2*^{-/-} mice as previous studies indicate using immobilization restrainers (Sim et al. 2013). However, *Drd2*^{-/-} mice showed similar results to WT on elevated-plus maze and Porsolt tests that are less stressful than long immobilization and restrained periods, indicating that active avoidance deficits cannot be explained only by differences in emotional responses.

Previous classical studies suggest that if learning does not occur in early trials, the animal can assess the situation as uncontrollable with a general decline in dopamine release that impairs the acquisition and hinders the establishment of new memories (Anisman 1977; Cabib and Puglisi-Allegra 1994). This could be related to the role of D₂Rs in tonic dopamine release and its high affinity for dopamine compared with other receptors like D₁R (Goto et al. 2007; Wall et al. 2011). Palmiter (2011) suggest that a failure in the maintenance of dopaminergic tone may reduce the levels of consciousness, inducing superficial information processing and consequently causing an important impairment in cognitive processes at different levels, similar to those observed in this study.

In addition, our results agree with previous studies that linked D₂R function in the striatum, amygdala and NAC to acquisition of aversive CRs (Nakanishi et al. 2014; Brandão et al. 2015; Slagter et al. 2015; Lenard et al. 2017; Blomeley et al. 2018; Iino et al. 2020). However, this study is the first of its type to demonstrate that the hippocampal D₂Rs are also essential for the acquisition and consolidation of associative memories.

Dopamine D₂Rs are Involved in Associative Learning and the Related Changes in Synaptic Strength at the Hippocampal CA3-CA1 Synapse

It is widely accepted that hippocampal circuits are involved in the acquisition of classically conditioned eyelid responses (Thompson 1988; Moyer et al. 1990; Ortiz et al. 2010; Gruart et al. 2015). Using in vivo recordings, hippocampal pyramidal cell firing in response to CS presentations increases across conditioning sessions (McEchron et al. 2003; Gruart et al. 2006, 2015; Madroñal et al. 2016). Eyeblink conditioning, an associative learning, induces a progressive increase in strength at the hippocampal CA3-CA1 synapse in awake mice (Gruart et al. 2006, 2015; Madroñal et al. 2007, 2016) that correlates with the increase in CRs across conditioning.

Previously, we convincingly demonstrated the functional relationships between LTP and Pavlovian conditioning (Gruart et al. 2006). In the present study, we decided to study D₂Rs

(white squares) group was also significantly larger than that presented by *Drd2*-siRNA (black squares) animals (*D*; **P* < 0.05). (E, F). Evolution of fEPSPs evoked at the CA3-CA1 synapse across conditioning for WT and *Drd2*^{-/-} mice (E) and for WT-Sham and *Drd2*-siRNA animals (F). fEPSP slopes are expressed as the percentage of fEPSP slope values collected during habituation sessions for each group. Differences in fEPSP slopes between WT and *Drd2*^{-/-} groups were statistically significant at the indicated sessions (E; **P* < 0.05), indicating that activity-dependent synaptic plasticity was severely impaired in both *Drd2*^{-/-} mice. No significant differences were found between the WT-Sham and *Drd2*-siRNA groups (*P* = 0.154).

in synaptic plasticity and same type of associative learning. Results shows that D₂Rs are necessary for the induction and maintenance of LTP at the CA3-CA1 synapse. Interestingly, input-output curves and paired-pulse potentiation evoked at this hippocampal synapse presented values in both *Drd2*^{-/-} and *Drd2*-siRNA mice similar to those reported in WT animals (Gruart et al. 2006; Madroñal et al. 2007). Thus, we can conclude that modified D₂Rs do not affect normal transmission in hippocampal synapses, but they significantly contribute to synaptic plasticity during experimentally evoked LTP as well as for the acquisition and storage of associative learning.

Results from LTP *in vivo* are related to results of previous classical *in vitro* studies that used the D₂R antagonist Domperidone finding no differences in LTP-induction, but abolishing the LTP maintenance (Dumwiddie et al. 1982; Frey et al. 1989, 1990). Also, studies in brain slices show that the genetic deletion or pharmacologic blockade of D₂R leads to the loss of LTP in ventral CA1 (Rocchetti et al. 2015).

Furthermore, our approach is unique because we simultaneously assess *Drd2*^{-/-} and hippocampal *Drd2*-siRNA mice during the processes of classical eyeblink conditioning and synaptic efficiency. We measured how the evoked extracellular fEPSPs change at the CA3-CA1 synapse during conditioning of behaving animals. Our data reveal a functional relationship between acquisition of associative learning and increase in synaptic strength at the CA3-CA1 synapse, showing that both are dramatically impaired when D₂R is eliminated or reduced.

Molecular Mechanisms of D₂R-Mediated Learning and Memory Processes

The molecular mechanism of D₂R mediating hippocampal synaptic transmission is not yet clear. It is possible that D₂R inactivation impairs NMDA-dependent LTP in CA1, corresponding with the remodeling of mesohippocampal dopamine fibers impairing learning and memory as we also demonstrated with D₁R inactivation (Suarez et al. 2020). Also, the loss of presynaptic control on dopamine levels in the absence of D₂R may produce an overactivation of postsynaptic D₁R and a decrement in DAT action (Ares-Santos et al. 2013; Rocchetti et al. 2015). In addition, previous studies indicate the presence of synergistic effects between D₁R and D₂R (Ichihara et al. 1992) that may result in the activation of a third intracellular signaling pathway by the Gq protein, increasing intracellular calcium levels (Lee et al. 2004; Hasbi et al. 2009). However, the existence of these heterodimers in hippocampal neurons is not yet proven.

Dopamine receptor-mediated effects can involve G β /G γ proteins (Missale et al. 1998; Beaulieu and Gainetdinov 2011) as well as other receptors. For example, D₂R forms a complex with A₂A receptors (Canals et al. 2003; Fuxe et al. 2005; Iino et al. 2020) and Sigma-1 receptors (Navarro et al. 2013) and recruits the AKT/GSK3 signaling pathways via cAMP-independent signaling mechanism (Beaulieu et al. 2005, 2007).

Conversely, neural calcium sensor 1 (NCS-1) regulates the D₂R phosphorylation interacting with GRK2. NCS-1 and D₂R have been shown to co-immunoprecipitate from mouse hippocampal lysates of CA1, CA3, and DG (Saab et al. 2009). NCS-1/D₂R interaction is critical for LTP facilitation in DG and underlies the promotion of specific forms of exploration essential for spatial memory (Kabbani et al. 2002) that would explain the deficits observed in the *Drd2*^{-/-} mice in this study.

In conclusion, we demonstrated that D₂R genetic deletion is sufficient to regulate hippocampal plasticity and spatial

and associative memories. In addition, with the use of siRNA-mediated KD, our results suggest an important role of D₂Rs in hippocampal memory, and help us understand cognitive alterations associated with neuropathologies such as PD.

Notes

We thank M. Esteban and E. Rubio for their technical assistance. The data presented in this paper was part of the PhD dissertation of I. Espadas available in open access at the Univ Complutense de Madrid (UCM).

Funding

Spanish Ministries of Science and Innovation (PID2019-111693RB-I00, PCIN-2015-098); Ramón Areces Foundation (ref 172275); European Union's Horizon 2020 research and innovation program, AND-PD (grant agreement no. 848002 to R.M., BFU2017-82375-R to A.G. and J.M.D.-G.); Health, Social Services and Equality (PI2019/09-3, CIBERNED CB06/05/0055 to R.M.); the Spanish Junta de Andalucía (BIO-122, PY18FR_823 to A.G. and J.M.D.-G.).

Conflicts of Interest

Nothing to report.

References

- Aarsland D, Creese B, Politis M, Chaudhuri KR, Fytche DH, Wintraub D, Ballard C. 2017. Cognitive decline in Parkinson disease. *Nat Rev Neurol*. 13:217–231.
- Alarcón JM, Malleret G, Touzani K, Vronskaya S, Ishii S, Kandel ER, Barco A. 2004. Chromatin acetylation, memory, and LTP are impaired in CBP^{+/-} mice: a model for the cognitive deficit in Rubinstein-Taybi syndrome and its amelioration. *Neuron*. 6:947–959.
- Anisman H. 1977. Time-dependent changes in activity, reactivity, and responsiveness during shock: effects of cholinergic and catecholaminergic manipulations. *Behav Biol*. 21:1–31.
- Ares-Santos S, Granado N, Moratalla R. 2013. The role of dopamine receptors in the neurotoxicity of methamphetamine. *J Intern Med*. 273:437–453.
- Ares-Santos S, Granado N, Espadas I, Martinez-Murillo R, Moratalla R. 2014. Methamphetamine causes degeneration of dopamine cell bodies and terminals of the nigrostriatal pathway evidenced by silver staining. *Neuropsychopharmacology*. 39:1066–1080.
- Avigan PD, Cammack K, Shapiro ML. 2020. Flexible spatial learning requires both the dorsal and ventral hippocampus and their functional interactions with the prefrontal cortex. *Hippocampus*. 30:733–734.
- Bamford NS, Wightman RM, Sulzer D. 2018. Dopamine's effects on corticostriatal synapses during reward-based behaviors. *Neuron*. 97:494–510.
- Beaulieu JM, Sotnikova TD, Marion S, Lefkowitz RJ, Gainetdinov RR, Caron MG. 2005. An Aky/beta-arrestin 2/PP2A signaling complex mediates dopaminergic neurotransmission and behavior. *Cell*. 122:261–273.
- Beaulieu JM, Tirota E, Sotnikova TD, Masri B, Salahpour A, Gainetdinov RR, Borrelli E, Caron MG. 2007. Regulation of Akt signaling by D2 and D3 dopamine receptors *in vivo*. *J Neurosci*. 27:881–885.

- Beaulieu JM, Gainetdinov RR. 2011. The physiology, signaling, and pharmacology of dopamine receptors. *Pharmacol Rev.* 63:182–217.
- Beeler JA, Faust RP, Turskson S, Ye H, Zhuang X. 2016. Low dopamine D₂ receptor increases vulnerability to obesity via reduced physical activity, not increased appetitive motivation. *Biol Psychiatry.* 79:887–897.
- Bethus I, Tse D, Morris RG. 2010. Dopamine and memory: modulation of the persistence of memory for novel hippocampal NMDA receptor-dependent paired associates. *J Neurosci.* 30:1610–1618.
- Blomeley C, Garau C, Burdakov D. 2018. Accumbal D₂ cells orchestrate innate risk-avoidance according to orexin signals. *Nat Neurosci.* 21:29–32.
- Brandão ML, de Oliveira AR, Muthuraju S, Colombo AC, Saito VM, Talbot T. 2015. Dual role of dopamine D₂-like receptors in the mediation of conditioned and unconditioned fear. *FEBS Lett.* 589:3433–3437.
- Broussard JI, Yang K, Levine AT, Tsetsenis T, Jenson D, Cao F, Garcia I, Arenkiel BR, Zhou FM, De Biasi M et al. 2016. Dopamine regulates aversive contextual learning and associated in vivo synaptic plasticity in the hippocampus. *Cell Rep.* 14:1930–1939.
- Cabib S, Puglisi-Allegra S. 1994. Opposite responses of mesolimbic dopamine system to controllable and uncontrollable aversive experiences. *J Neurosci.* 14:33–40.
- Canals M, Marcellino D, Fanelli F, Ciruela F, de Benedetti P, Goldberg SR, Neve K, Fuxe K, Agnati LF, Woods AS et al. 2003. Adenosine A_{2A}-dopamine D₂ receptor-receptor heteromerization: qualitative and quantitative assessment by fluorescence and bioluminescence energy transfer. *J Biol Chem.* 278:46741–46749.
- Christopher L, Marras C, Duff-Canning S, Koshimori Y, Chen R, Boileau I, Segura B, Monchi O, Lang AE, Rusian P et al. 2014. Combined insular and striatal dopamine dysfunction are associated with executive deficits in PD with mild cognitive impairment. *Brain.* 137:565–575.
- Christopher L, Marras C, Duff-Canning S, Koshimori Y, Chen R, Boileau I, Segura B, Monchi O, Lang AE, Rusian P et al. 2015. Combined insular and striatal dopamine dysfunction are associated with executive deficits in Parkinson's disease with mild cognitive impairment. *Brain.* 137:565–575.
- Da Cunha C, Mendes Angelucci ME, Canteras NS, Wonnacott S, Takahashi RN. 2002. The lesion of the rat substantia nigra pars compacta dopaminergic neurons as a model for Parkinson's disease memory disabilities. *Cell Mol Neurobiol.* 22:227–237.
- Danjo T, Yoshimi K, Funabiki K, Yawata S, Nakanishi S. 2014. Aversive behavior induced by optogenetic inactivation of ventral tegmental area dopamine neurons is mediated by dopamine D₂ receptors in the nucleus accumbens. *PNAS.* 111:6455–6460.
- Darvas M, Palmiter RD. 2009. Restriction of dopamine signaling to the dorsolateral striatum is sufficient for many cognitive behaviors. *Proc Natl Acad Sci USA.* 106:14664–14669.
- Darvas M, Palmiter RD. 2010. Restricting dopaminergic signaling to either dorsolateral or medial striatum facilitates cognition. *J Neurosci.* 30:58–65.
- Darvas M, Fadok JP, Palmiter RD. 2011. Requirement of dopamine signaling in the amygdala and striatum for learning and maintenance of a conditioned avoidance response. *Learn Mem.* 18:136–143.
- De Leonibus E, Pascucci T, Lopez S, Oliverio A, Amalric M, Mele A. 2007. Spatial deficits in a mouse model of Parkinson disease. *Psychopharmacology (Berl).* 194:517–525.
- Dumwiddie TV, Roverson NL, Worth T. 1982. Modulation of long-term potentiation: effects of adrenergic and neuroleptic drugs. *Pharmacol Biochem Behav.* 17:1257–1264.
- Edelmann E, Lessmann V. 2018. Dopaminergic innervation and modulation of hippocampal networks. *Cell Tissue Res.* 373:711–727.
- El-Ghundi M, Fletcher PJ, Drago J, Sibeley DR, BF O'D, George SR. 1999. Spatial learning deficit in dopamine D(1) receptor knockout mice. *Eur J Pharmacol.* 383:95–106.
- Espadas I, Darmopil S, Vergano-Vera E, Ortiz O, Oliva I, Vicario-Abejón C, Martín ED, Moratalla R. 2012. L-DOPA-induced increase in TH-immunoreactive striatal neurons in parkinsonian mice: insights into regulation and function. *Neurobiol Dis.* 48:271–281.
- Fadok JP, Dickerson TM, Palmiter RD. 2009. Dopamine is necessary for cue-dependent fear conditioning. *J Neurosci.* 29:11089–11097.
- Fetsko LA, Xu R, Wang Y. 2005. Effects of age and dopamine D₂L receptor-deficiency on motor and learning functions. *Neurobiol Aging.* 26:521–530.
- Franklin KBJ, Paxinos G. 2008. *The mouse brain in stereotaxic coordinates.* 3rd ed. Amsterdam: Elsevier.
- Frey U, Hartmann S, Mathies H. 1989. Domperidone, an inhibitor of the D₂-receptor blocks a late phase of an electrically induced long-term potentiation in the CA1-region in rats. *Biomed Biochem.* 7:473–476.
- Frey U, Schroeder H, Matthies H. 1990. Dopaminergic antagonists prevent long-term maintenance of posttetanic LTP in the CA1 region of rat hippocampal slices. *Brain Res.* 522:69–75.
- Fuxe K, Ferre S, Canals M, Torvinen M, Terasmaa A, Marcellino D, Goldberg SR, Staines W, Jacobsen KX, Lluís C et al. 2005. Adenosine A_{2A} and dopamine D₂ heteromeric receptor complexes and their function. *J Mol Neurosci.* 26:209–220.
- Gangarossa G, Longueville S, De Bundel D, Perroy J, Hervé D, Girault JA, Valjent E. 2012. Characterization of dopamine D₁ and D₂ receptor-expressing neurons in the mouse hippocampus. *Hippocampus.* 22:2199–2207.
- García-Sanz P, Orgaz L, Bueno-Gil G, Espadas I, Rodríguez-Traver E, Kulisevsky J, Gutierrez A, Davila JC, Gonzalez-Polo RA, Fuentes JM et al. 2017. N370S-GBA1 mutation causes lysosomal cholesterol accumulation in Parkinson's disease. *Mov Disord.* 32:1409–1422.
- Glickstein SB, Hof PR, Schmauss C. 2002. Mice lacking dopamine D₂ and D₃ receptors have spatial working memory deficits. *J Neurosci.* 22:5619–5629.
- Goto Y, Grace AA. 2005. Dopaminergic modulation of limbic and cortical drive of nucleus accumbens in goal-directed behavior. *Nat Neurosci.* 8:805–812.
- Goto Y, Otani S, Grace AA. 2007. The ying and yang of dopamine release: a new perspective. *Neuropharmacology.* 53:83–87.
- Granado N, Ortiz O, Suárez LM, Martín ED, Ceña V, Solís JM, Moratalla R. 2008. D₁ but not D₅ dopamine receptors are critical for LTP, spatial learning, and LTP-induced arc and zif268 expression in the hippocampus. *Cereb Cortex.* 18:1–12.
- Granado N, Lastres-Becker I, Ares-Santos S, Oliva I, Martín E, Cuadrado A, Moratalla R. 2011. Nrf2 deficiency potentiates methamphetamine-induced dopaminergic axonal damage and gliosis in the striatum. *Glia.* 59:1850–1863.

- Grace AA, Floresco SB, Goto Y, Lodge DJ. 2007. Regulation of firing of dopaminergic neurons and control of goal-directed behaviors. *Trends Neurosci.* 30:220–227.
- Groessi F, Munsch T, Meis S, Griessner J, Kaczanowska J, Pliota P, Kargi D, Badurek S, Kraitsy K, Rassoulpour A et al. 2018. Dorsal tegmental dopamine neurons gate associative learning of fear. *Nat Neurosci.* 21:952–962.
- Grogan JP, Knight LE, Smith L, Irigoras Izagirre N, Howat A, Knight BE, Bickerton A, Isotalus HK, Coulthard EJ. 2018. Effects of Parkinson's disease and dopamine on digit span measures of working memory. *Psychopharmacology (Berl).* 235:3443–3450.
- Gruart A, Muñoz MD, Delgado-García JM. 2006. Involvement of the CA3-CA1 synapse in the acquisition of associative learning in behaving mice. *J Neurosci.* 26:1077–1087.
- Gruart A, Sánchez-Campusano R, Fernández-Guizán A, Delgado-García JM. 2015. A differential and timed contribution of identified hippocampal synapses to associative learning in mice. *Cereb Cortex.* 5:2542–2555.
- Gureviciene I, Ikonen S, Gurevicius K, Sarkaki A, van Groen T, Pussinen R, Ylilinen A, Tanila H. 2004. Normal induction but accelerated decay of LTP in APP + PS1 transgenic mice. *Neurobiol Dis.* 15:188–195.
- Handler A, Graham TGW, Cohn R, Morante I, Siciliano AF, Zeng J, Li Y, Ruta V. 2019. Distinct dopamine receptor pathways underlie the temporal sensitivity of associative learning. *Cell.* 178:60–75.
- Hasbi A, Fan T, Alijaniam M, Nguyen T, Perreault ML, O'Dowd BF, George SR. 2009. Calcium signaling cascade links dopamine D1-D2 receptor heteromer to striatal BDNF production and neuronal growth. *PNAS.* 106:21377–21382.
- Higuera-Matas A, Botreau F, Del Olmo N, Miguéns M, Olías O, Montoya GL, García-Lecumberri C, Ambrosio E. 2010. Peri-adolescent exposure to cannabinoids alters the striatal and hippocampal dopaminergic system in the adult rat brain. *Eur Neuropharmacol.* 20:895–906.
- Ichihara K, Nabeshima T, Kameyama T. 1992. Effects of dopamine receptor agonists on passive avoidance learning in mice: interaction of dopamine D1 and D2 receptors. *Eur J Pharmacol.* 213:243–249.
- Iino Y, Sawada T, Yamaguchi K, Tajiri M, Ishii S, Kasai H, Yagishita S. 2020. Dopamine D2 receptors in discrimination learning and spine enlargement. *Nature.* 579:555–560.
- Ishikawa K, Otto T, McGaugh JL. 1982. Evidence for dopamine as a transmitter in dorsal hippocampus. *Brain Res.* 232:222–226.
- Kabbani N, Negyessy L, Lin R, Goldman-Rakic P, Levenson R. 2002. Interaction with neuronal calcium sensor NCS-1 mediates desensitization of the D2 dopamine receptor. *J Neurosci.* 22:8476–8486.
- Kempadoo KA, Mosharov EV, Choi SJ, Sulzer D, Kandel ER. 2016. Dopamine release from the locus coeruleus to the dorsal hippocampus promotes spatial learning and memory. *PNAS.* 113:14835–14840.
- Kemppainen N, Laine M, Laakso MP, Kaasinen V, Nagren K, Vahlberg T, Kurki T, Rinne JO. 2003. Hippocampal dopamine D2 receptors correlate with memory functions in Alzheimer's disease. *Eur J Neurosci.* 18:149–154.
- Kravitz AV, Freeze BS, Parker PR, Kay K, Thwin MT, Deisseroth K, Kreitzer AC. 2010. Regulation of parkinsonian motor behaviors by optogenetic control of basal ganglia circuitry. *Nature.* 466:622–626.
- Lee SP, So CH, Rashid AJ, Varghese G, Cheng R, Lança AJ, BF O'D, George SR. 2004. Dopamine D1 and D2 receptor co-activation generates a novel phospholipase C-mediated calcium signal. *J Biol Chem.* 279:35671–35678.
- Lenard L, Ollmann T, Laszlo K, Kovacs A, Galosi R, Kallai V, Attila T, Kertes E, Zagoracz O, Karadi Z et al. 2017. Role of D2 dopamine receptors of the ventral pallidum in inhibitory avoidance learning. *Behav Brain Res.* 321:99–105.
- Linden J, James AS, McDaniel C, Jentsch JD. 2018. Dopamine D2 receptors in dopaminergic neurons modulate performance in a reversal learning task in mice. *eNeuro.* 5:0229–0217.
- Madroñal N, Delgado-García JM, Gruart A. 2007. Differential effects of long-term potentiation evoked at the CA3 CA1 synapse before, during, and after the acquisition of classical eyeblink conditioning in behaving mice. *J Neurosci.* 27:12139–12146.
- Madroñal N, Delgado-García JM, Fernández-Guizán A, Chatterjee J, Köhn M, Mattucci C, Jain A, Tsetsenis T, Illarionova A, Grinevich V et al. 2016. Rapid erasure of hippocampal memory following inhibition of dentate gyrus granule cells. *Nat Commun.* 7:10923.
- Mansikka H, Erbs E, Borrelli E, Pertovaara A. 2005. Influence of the dopamine D2 receptor knockout on pain-related behavior in the mouse. *Brain Res.* 1052:82–87.
- Martin SJ, Morris RG. 2002. New life in an old idea: the synaptic plasticity and memory hypothesis revisited. *Hippocampus.* 12:609–636.
- Matamala M, McGovern AE, Mi JD, Mazzone SB, Balleine BW, Bertran-Gonzalez J. 2020. Local D2-to D1-neuron transduction updates goal-directed learning in the striatum. *Science.* 367:549–555.
- McEchron MD, Tseng W, Disterhoft JF. 2003. Single neurons in CA1 hippocampus encode trace interval duration during trace heart rate (fear) conditioning in rabbit. *J Neurosci.* 23:1535–1547.
- McNamara CG, Tejero-Cantero A, Trouche S, Campo-Urriza N, Dupret D. 2014. Dopaminergic neurons promote hippocampal reactivation and spatial memory persistence. *Nat Neurosci.* 17:1658–1660.
- Missale C, Nash SR, Robinson SW, Jaber M, Caron MG. 1998. Dopamine receptors: from structure to function. *Physiol Rev.* 78:189–225.
- Moratalla R, Vallejo M, Elibol B, Graybiel AM. 1996. D1-class dopamine receptors influence cocaine-induced persistent expression of Fos-related proteins in striatum. *Neuroreport.* 8:1–5.
- Moyer JR, Deyo RA, Disterhoft JF. 1990. Hippocampectomy disrupts trace eye-blink conditioning in rabbits. *Behav Neurosci.* 104:243–252.
- Mura A, Feldon J. 2003. Spatial learning in rats is impaired after degeneration of the nigrostriatal dopaminergic system. *Mov Disord.* 18:860–871.
- Nakamura T, Sato A, Kitsukawa T, Momiyama T, Yamamori T, Sasaoka T. 2014. Distinct motor impairments of dopamine D1 and D2 receptor knockout mice revealed by three types of motor behavior. *Front Integr Neurosci.* 8:56.
- Nakanishi S, Hikida T, Yawata S. 2014. Distinct dopaminergic control of the direct and indirect pathways in reward-based and avoidance learning behaviors. *Neuroscience.* 282C:49–59.
- Navarro G, Moreno E, Bonaventura J, Brugarolas M, Farré D, Aquinaga D, Mallol J, Cortés A, Casadó V, Lluís C et al. 2013. Cocaine inhibits dopamine D2 receptor signaling via sigma-1-D2 receptor heteromers. *Plos One.* 8:e61245.

- Nguyen CL, Tran AH, Matsumoto J, Hori E, Uwano T, Ono T, Nishijo H. 2014. Hippocampal place cell responses to distal and proximal cue manipulations in dopamine D₂ receptor-knockout mice. *Brain Res.* 1567:13–27.
- Nyberg L, Karalija N, Salami A, Andersson M, Wahlin A, Kaboovand N, Kohncke Y, Axelsson J, Rieckmann A, Papenberger G et al. 2016. Dopamine D₂ receptor availability is linked to hippocampal-caudate functional connectivity and episodic memory. *PNAS.* 113:7918–7923.
- O'Carroll CM, Martin SJ, Sandin J, Frenguelli B, Morris RGM. 2006. Dopaminergic modulation of the persistence of one-trial hippocampus-dependent memory. *Learn Mem.* 13:760–769.
- Olivetti PR, Balsam PD, Simpson EH, Kellendonk C. 2020. Emerging roles of striatal dopamine D₂ receptors in motivated behavior: implications for psychiatric disorders. *Basic Clin Pharmacol Toxicol.* 126:47–55.
- Ortiz O, Delgado-García JM, Espadas I, Bahí A, Trullas R, Dreyer JL, Gruart A, Moratalla R. 2010. Associative learning and CA3-CA1 synaptic plasticity are impaired in D1R null, D1R knockout mice and in hippocampal siRNA silenced DR1a mice. *J Neurosci.* 30:12288–12300.
- Palminter RD. 2011. Dopamine signaling as a neural correlate of consciousness. *Neuroscience.* 198:213–220.
- Pavón N, Martín AB, Mendiadua A, Moratalla R. 2006. ERK phosphorylation and FosB expression are associated with L-DOPA-induced dyskinesia in hemiparkinsonian mice. *Biol Psychiatry.* 59:64–74.
- Piggott MA, Ballard CG, Rowan E, Holmes C, McKeith IG, Jaros E, Perry RH, Perry EK. 2007. Selective loss of dopamine D₂ receptors in temporal cortex in dementia with Lewy bodies, association with cognitive decline. *Synapse.* 61:903–911.
- Puighermanal E, Castell L, Esteve-Codina A, Melser S, Kaganovsky K, Zussy C, Boubaker-Vitre J, Gut M, Rialle S, Kellendonk C et al. 2020. Functional and molecular heterogeneity of D₂R neurons along dorsal ventral axis in the striatum. *Nat Commun.* 11:1957.
- Pittenger C, Fasano S, Mazzocchi-Jones D, Dunnett SB, Kandel ER, Brambilla R. 2006. Impaired bidirectional synaptic plasticity and procedural memory formation in striatum-specific cAMP response element-binding protein-deficient mice. *J Neurosci.* 10:2808–2813.
- Porsolt RD, Bertin A, Jalfre M. 1978. Behavioral despair in rats and mice: strain differences and the effects of imipramine. *Eur J Pharmacol.* 51:291–294.
- Rocchetti J, Isingrini E, Dal Bo G, Sagheby S, Menegaux A, Tronche F, Levesque D, Moquin L, Gratton A, Wong TP et al. 2015. Presynaptic D₂ dopamine receptors control long-term depression expression and memory processes in the temporal hippocampus. *Biol Psychiatry.* 77:513–525.
- Rosen ZB, Cheung S, Siegelbaum SA. 2015. Midbrain dopamine neurons bidirectionally regulate CA3-CA1 synaptic drive. *Nat Neurosci.* 18:1763–1771.
- Ruiz-De Diego I, Mellstrom B, Vallejo M, Naranjo JR, Moratalla R. 2014. Activation of DREAM (downstream regulatory element antagonistic modulator), a calcium-binding protein, reduces L-DOPA-induced dyskinesias in mice. *Biol Psychiatry.* 77:95–105.
- Saab BJ, Georgiou J, Nath A, Lee FJ, Wang M, Michalon A, Liu F, Mansuy IM, Roder JC. 2009. NCS-1 in the dentate gyrus promotes exploration, synaptic plasticity, and rapid acquisition of spatial memory. *Neuron.* 63:643–656.
- Seligman ME, Rosellini RA, Kozak MJ. 1975. Learned helplessness in the rat: time course, immunization, and reversibility. *J Comp Physiol Psychol.* 88:542–547.
- Sim HR, Choi TY, Lee HJ, Kang EY, Yoon S, Han PL, Choi SY, Baik JH. 2013. Role of dopamine D₂ receptors in plasticity of stress-induced addictive behaviours. *Nat Commun.* 4:1579.
- Slagter HA, Georgopoulou K, Frank MJ. 2015. Spontaneous eye blink rate predicts learning from negative, but not positive, outcomes. *Neuropsychologia.* 71:126–132.
- Smith CC, Greene RW. 2012. CNS dopamine transmission mediated by noradrenergic innervation. *J Neurosci.* 2:6072–6080.
- Schneider JS, Roeltgen DP. 1993. Delayed matching-to-sample, object retrieval and discrimination reversal deficits in chronic low dose MPTP-treated monkeys. *Brain Res.* 615:351–354.
- Setlow B, McGaugh JL. 1999. Involvement of the posteroventral caudate-putamen in memory consolidation in the Morris water maze. *Neurobiol Learn Mem.* 71:240–247.
- Setlow B, McGaugh JL. 2000. D₂ dopamine receptor blockade immediately post-training enhances retention in hidden and visible platform versions of the water maze. *Learn Mem.* 7:187–191.
- Soares-Cunha C, Coimbra B, David-Pereira A, Borges S, Pinto L, Costa P, Sousa N, Rodrigues AJ. 2016. Activation of D₂ dopamine receptor-expressing neurons in the nucleus accumbens increases motivation. *Nat Commun.* 7:11829.
- Solis O, Espadas I, Del-Bel EA, Moratalla R. 2015. Nitric oxide synthase inhibition decreases L-DOPA-induced dyskinesia and the expression of striatal molecular markers in Pitx3 (–/–) aphakia mice. *Neurobiol Dis.* 73:49–59.
- Solis O, Garcia-Sanz P, Martin AB, Granado N, Sanz-Magro A, Podlesniy P, Trullas R, Murer MG, Maldonado R, Moratalla R. 2019. Behavioral sensitization and cellular responses to psychostimulants are reduced in D₂R knockout mice. *Addict Biol.* 12:e12840.
- Suarez LM, Solis O, Sanz-Magro A, Alberquilla S, Moratalla R. 2020. Dopamine D₁ receptors regulate spines in striatal direct-pathway and indirect-pathway neurons. *Mov Disord.* 35:1810–1821.
- Tanaka Y, Meguro K, Yamaguchi S, Ishii H, Watanuki S, Funaki Y, Yamaguchi K, Yamadori A, Iwata R, Itoh M. 2003. Decreased striatal D₂ receptor density associated with severe behavioral abnormality in Alzheimer's disease. *Ann Nucl Med.* 17:567–573.
- Takatsuki K, Kawahara S, Kotani S, Fukunaga S, Mori H, Mishina M, Kirino Y. 2003. The hippocampus plays an important role in eyeblink conditioning with a short trace interval in glutamate receptor subunit delta 2 mutant mice. *J Neurosci.* 23:17–22.
- Takeuchi T, Duzskiewicz AJ, Sonneborn A, Spooner PA, Yamasaki M, Watanabe M, Smith CC, Fernandez G, Deisseroth K, Greene RW et al. 2016. Locus coeruleus and dopaminergic consolidation of everyday memory. *Nature.* 537:357–362.
- Thompson RF. 1988. The neural basis of basic associative learning of discrete behavioral responses. *Trends Neurosci.* 11:152–155.
- Wall VZ, Parker JG, Fadok JP, Darvas M, Zweifel L, Palminter RD. 2011. A behavioral genetics approach to understanding D₁ receptor involvement in phasic dopamine signaling. *Mol Cell Neurosci.* 46:21–31.

- Wang SH, Redondo RL, Morris RG. 2010. Relevance of synaptic tagging and capture to the persistence of long-term potentiation and everyday spatial memory. *Proc Natl Acad Sci USA*. 107:19537–19542.
- Wei X, Ma T, Cheng Y, Huang CCY, Wang X, Lu J, Wang J. 2018. Dopamine D1 or D2 receptor-expressing neurons in the central nervous system. *Addict Biol*. 23: 569–584.
- Weintraub D, Simuni T, Caspell-Garcia C, Coffey C, Lasch S, Siderowf A, Aarsland D, Barone P, Burn D, Chahine LM et al. 2015. Cognitive performance and neuropsychiatric symptoms in early, untreated Parkinson's disease. *Mov Disord*. 30:919–927.
- Xing B, Kong H, Meng X, Wei SG, Xu M, Li SB. 2010. Dopamine D1 but not D3 receptor is critical for spatial learning and related signaling in the hippocampus. *Neuroscience*. 169:1511–1519.